# The Influence of Bed Roughness and Sediment Supply on Alluvial Cover in Bedrock Channels

Jagriti Mishra[1], Takuya Inoue[1]

[1] Civil Engineering Research Institute for Cold Region, Sapporo-Hokkaido, Japan

*Correspondence to*: Jagriti Mishra (jagritimp@gmail.com)

**Abstract.** Several studies have implied towards the importance of bedrock-bed roughness on alluvial cover; besides, several mathematical models have also been introduced to mimic the effect bed roughness may project on alluvial cover in bedrock channels. Here, we provide an extensive review of research exploring the relationship between alluvial cover, sediment supply and bed topography of bedrock channels, thereby, describing various mathematical models used to analyse deposition of alluvium. In the interest of analysing the efficiency of various available mathematical models, we performed a series of laboratory-scale experiments with varying bed roughness and compared the results with various models. Our experiments show that alluvial cover is not merely governed by increasing sediment supply, and, bed topography is an important controlling factor of alluvial cover. We tested five theoretical models with the experimental results and the results suggest a fit of certain models for a particular bed topography and inefficiency in predicting higher roughness topography. Three models efficiently predict the experimental observations, albeit their limitations.

## 1 Introduction

Economic growth worldwide has fuelled the demand for the construction of straightened river channels, sabo dams, the collection of gravel samples for various research, etc., leading to a decline in sediment availability and alluvial bed cover. Sumner et al. (2019) reported that the straightening of the Yubari River, which was carried out to improve the drainage of farmland, caused the bedrock to be exposed and the knickpoint to migrate upstream. In addition, construction of a dam in the upstream section of Toyohira river in Hokkaido – Japan, decreased the sediment availability to the downstream section contributing to the formation of a knickpoint (Yamaguchi et al. 2017 in Japanease). Sediment availability plays a very important role in controlling the landscape evolution and determining the morphology of the river over geologic time (Moore 1926; Shepherd 1972). Various field-scale (Gilbert, 1877; Shepherd, 1972; Turowski et al., 2008b; Turowski and Rickenmann, 2009; Johnson et al., 2010; Jansen et al., 2011; Cook et al., 2013; Inoue et al., 2014; Beer and Turowski, 2015; Beer et al., 2017), laboratory-scale (Sklar and Dietrich, 1998, 2001; Chatanantavet and Parker, 2008; Finnegan et al., 2007; Johnson and Whipple, 2010, 2007; Hodge and Hoey, 2016a, 2016b; Hodge et al., 2016; Turowski and Bloem, 2016; Inoue et al., 2017b, Mishra et al., 2018; Fernandez et al., 2019; Inoue and Nelson, 2020), and theoretical and numerical studies (Hancock and Anderson, 2002; Sklar and Dietrich, 2004, 2006; Lague, 2010; Hobley et al., 2011; Nelson and Seminara, 2011, 2012; Johnson, 2014; Nelson et al., 2014; Zhang et al., 2015; Inoue et al. 2016, 2017a; Turowski and Hodge 2017; Turowski, 2018) have suggested that sediment availability has two contradicting effects on the river bed, known as Tools and Cover effect. It acts as a tool and erodes the bedrock bed, known as tools effect. As sediment availability increases, the sediment starts settling down on the river bed providing a cover for the bed underneath from further erosion, known as the cover effect.

Sklar and Dietrich (2001) and Scheingross et al., (2014) performed rotary-abrasion mill experiments showing the importance of cover in controlling incision rates in bedrock channels. Reach scale studies of Erlenbach performed by Turowski et al. (2013) showed how extreme flood events can contribute to incision by ripping off the channel's alluvial cover. Cook et al. (2013) suggested that bedrock incision rates were dominantly controlled by the availability of bedload. Their field surveys of bedrock gorge cut by Daán River in Taiwan showed that the channel bed merely eroded for years, despite floods and available

suspended sediment. Channel incision occurred only when bedload tools became available. Yanites et al. (2011) studied the changes in the Peikang River in central Taiwan triggered by the thick sediment cover introduced by landslides and typhoons during the 1999 Chi-Chi earthquake. Their results show slowed or no incision in high transport capacity and low transport capacity channels. Mishra et al. (2018) showed that incision rate increased when the sediment supply rate of the laboratory-scale channel became considerably smaller than the sediment carrying capacity of the channel. Laboratory scale experiments performed by Shepherd and Schumm (1974), Wohl and Ikeda (1997) and Inoue and Nelson (2020) showed formation of several longitudinal grooves at low sediment supply to capacity ratio. As the sediment supply increases, one of the grooves attracts more sediment supply and progresses into a comparatively straight, wide and shallow inner channel which further progresses into a narrower, more sinuous, deeper inner channel (Wohl and Ikeda, 1997; Inoue et al., 2016). Channels with higher sediment supply to capacity ratio are expected to be wider as alluvial cover shifts erosion from bed to banks of the channel (Beer et al. 2016; Turowski et al., 2008a and Whitbread et al., 2015). These findings show the ratio of sediment supply to capacity controls alluvial cover ratio, bedrock incision rate and morphodynamics in bedrock rivers.

Finnegan et al. (2007) conducted laboratory-scale experiments and studied the interdependence among incision, bed roughness and alluvial cover. Their results indicated that alluvial deposition on the bed shifted bed erosion to higher regions of the channel or bank of the channel. Similar findings were noted in flume studies conducted by Wohl and Ikeda (1997) and Johnson and Whipple (2010). They have shown the importance of alluvial cover in regulating the roughness of bedrock bed by providing a cover for the local lows and thereby inhibiting the erosion and focusing erosion on local highs. Inoue et al. (2014) conducted experiments by excavating channel into natural bedrocks in Ishikari River, Asahikawa, Hokkaido – Japan. They conducted experiments with different combinations of flow discharge, sediment supply rate, grain size and roughness. Their experiments advocated that the dimensionless critical shear stress for sediment movement on bedrock is related to the roughness of the channel. Their experiments also suggested that with an increase in alluvial cover, the relative roughness (i.e., the ratio of bedrock hydraulic roughness to moving sediment size) decreases, also, erosion in areas with an exposed bed is proportionate to sediment flux. Fuller et al. (2016) performed laboratory scale experiments and established the importance of bed-roughness in determining the incision and lateral erosion rates. Chatanantavet and Parker (2008) conducted laboratory-scale experiments in straight concrete bedrock channels with varying bedrock roughness and evaluated bedrock exposure with respect to sediment availability. In their experiments, alluvial cover increased linearly with increasing sediment supply in case of higher bed roughness, whereas in case of lower bed roughness and higher slopes, the bed shifted abruptly from being completely exposed to being completely covered. This process of the bedrock bed suddenly becoming completely alluvial from being completely exposed is known as rapid alluviation. Rapid alluviation was also observed in the laboratory scale experiment conducted by Hodge and Hoey (2016a; 2016b) in a 3D printed flume of natural stream Trout Beck, North Pennies-U.K. Their first set of experiments focused on quantifying hydraulic change with varying discharge, suggesting that hydraulic properties fluctuate more during higher discharge. Their second set of experiments (Hodge and Hoey, 2016b) concentrated on quantifying the sediment dynamics for varying discharge and sediment supply. They supplied 4 kg and 8 kg of sediment pulse to the channel and observed a similar alluvial pattern in both cases suggesting that the deposition of sediment on the bed may not only depend on the amount of sediment supplied, but may be strongly influenced by the bed topography and roughness. The latest studies of alluvial cover in bedrock rivers have entered the next stage, which includes not only the effect of sediment supply-capacity ratio but also the effect of bed roughness.

A majority of traditional bed-erosion models are classified as the stream power and shear stress family of models (cf. Shobe et al., 2017; Turowski, 2018) (e.g., Howard, 1994; Whipple and Tucker, 1999), in which bed erosion is a function of discharge and bed-slope. These models however cannot describe the role of sediment in controlling the bed dynamics. Several models remedy this shortcoming by considering the tools and cover effect of sediment supply (Sklar and Dietrich, 1998, 2004; Turowski et al., 2007; Chatanantavet and Parker, 2009; Hobley et al., 2011; Inoue et al., 2017b). In section 1.1, we introduce

previous theoretical and numerical models that take into account sediment cover in bedrock channel. In sections 1.2 to 1.6, we describe in detail the governing equations of the five models dealt with in this study.

### 1.1 Previous Models for Sediment Cover

One of the simplest and first models to incorporate effects of sediment availability and transport capacity of the channel was introduced by Sklar and Dietrich (1998; 2004). According to saltation-abrasion model proposed by Sklar and Dietrich (1998; 2004), the alluvial cover $P_c$ increases linearly with the ratio of sediment supply to sediment transport capacity $q_{bs}/q_{bc}$, i.e. in absence of sediment supply, the alluvial cover is absent. However, when sediment supply becomes equal to or exceeds the transport capacity of the channel, the channel bed is fully covered. In order to express the non-linear relationship between $P_c$ and $q_{bs}/q_{bc}$, Turowski et al. (2007) proposed a model that considered the cover effect as an exponential function of the ratio of sediment flux to sediment transport capacity. The model uses a probabilistic argument i.e., when sediment supply is less than the capacity of the channel, grains have an equal probability of settling down over any part of the bed. Also, the deposited grains can be static or mobile. These models however lack the statement of sediment mass conservation. A group of models utilise entrainment/deposition flux or Exner equation for sediment mass conservation (Turowski, 2009; Lague, 2010; Inoue et al., 2014;2016;2017; Nelson and Seminara, 2012; Hodge and Hoey, 2012; Johnson, 2014; Zhang, 2015; Turowski and Hodge, 2017).

Turowski and Hodge (2017) generalized the arguments presented by Turowski et al. (2007) and Turowski (2009), and proposed a reach- scale probability-based model that can deal with the evolution of cover residing on the bed and the exposed bedrock. Turowski (2018) proposed a model and linked availability of cover in regulating the sinuosity of the channel.

Lague (2010) employed Exner equation to calculate alluvial thickness with respect to average grain size $d$. Their model however lacks the tools effect for bed erosion. Recently, Johnson (2014) and Inoue et al. (2014) proposed reach-scale physically-based models that could encompass the effects of bed roughness in addition to alluvial thickness. Inoue et al. (2014) also conceptualised 'Clast Rough' and 'Clast Smooth' bedrock surfaces. A bedrock surface is clast-rough when bedrock hydraulic roughness is greater than the alluvial bed hydraulic roughness (supplied sediment), otherwise, a surface is clast-smooth i.e. when the bedrock roughness is lower than the alluvial roughness. Inoue et al. (2014) and Johnson (2014) clarified that the areal fraction of alluvial cover exhibits a hysteresis with respect to the sediment supply and transport ratio in a clast smooth bedrock channel. They described that along with rapid alluviation, perturbations in sediment supply can also lead to rapid entrainment. Whether the bed undergoes rapid alluviation or rapid entrainment is determined by the bed condition when perturbations in sediment supply occur. If the perturbations occur on an exposed bed, it undergoes rapid alluviation, conversely, when perturbations happen on an alluviated bed, it undergoes rapid entrainment. Zhang et al. (2015) proposed macro-roughness saltation-abrasion model (MRSA) in which cover is a function of alluvial thickness and macro-roughness height. Nelson and Seminara (2012) proposed a linear stability analysis model for the formation of alternate bars on bedrock bed. Inoue et al. (2016) expanded Inoue et al. (2014) to allow variations in the depth and width of alluvial thickness in the channel cross-section. They further modified the numerical model (Inoue et al., 2017a) and implemented the model to observe changes in a meander bend.

Hodge and Hoey (2012) introduced reach-scale Cellular Automaton Model that assigned an entrainment probability to each grain. The assigned probability of each grain was decided by the number of neighbouring cells containing a grain. If five or more of total eight neighbouring cells contained grain, the grain was considered to be a part of the cover, otherwise, it was considered an isolated grain. They suggested that rapid alluviation occurred only in cases when isolated grains were more than the cover on the bed. Also, they advised a sigmoidal relationship between $q_{bs}/q_{bc}$ and $1 - P_c$. Aubert et al. (2016) proposed a Discrete-Element Model where they determined $P_c$ from the velocity distribution of the grains. If the velocity of a grain is $1/10^{th}$ or lower than the maximum velocity, the grain settles as cover on the bedrock surface. The model, however, cannot deal with non-uniform velocity fields and hence cannot predict results for varying alluvial cover.

Except for the Lagrangian description models that track individual particles (i.e., Hodge and Hoey, 2012; Aubert et al., 2016), the Eulerian description models are roughly classified into four categories; the linear model proposed by Sklar and Dietrich (1998, 2004), the exponential model proposed by Turowski et al. (2007), the probabilistic model proposed by Turowski and Hodge (2017) and the roughness models proposed by Inoue et al. (2014), Johnson (2014), Nelson and Seminara (2012) and Zhang et al. (2015). In this study, we focus on a detailed study of the similarities and differences among the Eulerian description models proposed by Sklar and Dietrich (2004), Turowski et al. (2007), Inoue et al. (2014), Johnson (2014) and Turowski and Hodge (2017). We compare the efficacy of these models from comparisons with our experimental results. In addition, we apply the roughness models (Inoue et al., 2014; Johnson, 2014) to the experiments conducted by Chatanantavet and Parker (2008) in order to analyse the effect of bedrock roughness on alluvial cover in a mixed bedrock - alluvial river with alternate bars.

### 1.2 Linear Model

The value of $P_c$ i.e. the alluvial cover ratio is 1 when the sediment supply is larger than the transport capacity, the alluvial cover does not decrease as the sediment gets deposited on the bed, consequently, the bedrock is not exposed. If there is no sediment supply, the sediment deposit will disappear and eventually, the bedrock bed will be completely exposed and $P_c$ will be equal to 0. Sklar and Dietrich (2004) lineally connected these two situations, and proposed a linear model to include the Cover effect in their saltation – abrasion model;

$$P_c = \begin{cases} q_{bs}/q_{bc} & for\ \ 0 \le q_{bs}/q_{bc} \le 1 \\ 1 & for\ \ q_{bs}/q_{bc} > 1 \end{cases} \quad (1)$$

where, $P_c$ is the mean areal fraction of alluvial cover, $q_{bs}$ and $q_{bc}$ are the volume sediment supply rate per unit width and transport capacity, respectively.

### 1.3 Exponential Model

Turowiski (2007) assumed that the sediment mass ratio is equal to the ratio of sediment supply to capacity, and derived the following exponential model using a probabilistic argument;

$$P_c = 1 - \exp\left(-\varphi \frac{q_{bs}}{q_{bc}}\right) \quad (2)$$

where, $\varphi$ is a dimensionless cover factor parameter and determines sediment deposition on covered areas for $\varphi < 1$ and deposition on uncovered areas for $\varphi > 1$ (Turowski et al., 2007; Turowski, 2009). Note that their assumption was demonstrated to be incorrect by the recent analysis of Turowski and Hodge (2017).

### 1.4 Macro Roughness Model

The experimental results of Inoue et al. (2014) motivated their mathematical model formulating the interaction between alluvial cover, dimensionless critical shear stress, transport capacity and the ratio of bedrock hydraulic roughness to alluvial hydraulic roughness. They calculated total hydraulic roughness height ($k_s$) as a function of alluvial cover:

$$k_s = \begin{cases} (1 - P_c)k_{sb} + (P_c)k_{sa} & for\ \ 0 \le P_c \le 1 \\ k_{sa} & for\ \ P_c > 1 \end{cases} \quad (3)$$

where $k_s$ is the total hydraulic roughness height of bedrock channel, $P_c$ is the cover fraction calculated as proposed by Parker et al. (2013) depends on ratio $\eta_a/L$ where $\eta_a$ is the alluvial cover thickness and $L$ is the bedrock macro-roughness height (i.e. topographic unevenness of the bed). $k_{sb}$ and $k_{sa}$(= 1 – 4 d, here set to 2) represent the hydraulic roughness height of bedrock and alluvial bed respectively. The total transport capacity per unit width $q_{bc}$ in Inoue et al.'s model is calculated as follows:

$$q_{bc} = \alpha(\tau_* - \tau_{*c})^{1.5}\sqrt{Rgd^3} \quad (4)$$

$$\tau_{*c} = 0.027(k_s/d)^{0.75} \quad (5)$$

where $\alpha$ is a bedload transport coefficient taken as 2.66 in this study, $\tau_*$ and $\tau_{*c}$ are the dimensionless shear stress and dimensionless critical shear stress, $R$ is the specific gravity of the sediment in water (1.65), $g$ is the gravitational acceleration and $d$ is the particle size. In this model, $P_c$ is back-calculated from Equations (3), (4) and (5) under the assumption that the sediment supply rate $q_{bs}$ and the sediment transport capacity $q_{bc}$ are balanced in dynamic equilibrium state.

The sensitivity analysis of bedrock roughness and sediment supply rate conducted by Inoue et al. (2014) showed that for a given sediment supply, the deposition ($P_c$) is higher when bedrock roughness is larger. They also showed that clast-smooth surface shows a sudden transition from completely exposed bedrock to completely alluvial, i.e., clast-smooth surfaces show rapid alluviation.

### 1.5 Surface Roughness Model

Johnson (2014) proposed a roughness model using the median diameter grain size. They also calculated the hydraulic roughness using the aerial alluvial cover fraction.

$$k_{sa} = r_d d[1 + (k_{\#D} - 1)P_c] \quad (6)$$

where $r_d = 2$ is a coefficient and $k_{\#D}$ is called a non-dimensional alluvial roughness representing variations in topography. For a fully alluviated bed, $k_{sa}$=2d. The bedrock hydraulic roughness** $k_{sb} = r_d r_{br}\sigma_{br}$ where $r_{br}$ is a scaling parameter for bedrock roughness to grain roughness and $\sigma_{br}$ is the bedrock surface roughness. Their model calculates bedrock shear stress using Wilcock and Crowe (2003) hiding/exposure function ($b_r$), modified to depend on a standard deviation of bedrock elevations and a bedrock roughness scaling parameter. Johnson (2014) calculated the total transport capacity using bedload equations proposed by Meyer-Peter and Müller (1948) and Wilcock and Crowe (2003). Here we introduce Meyer-Peter and Müller (MPM) based Johnson's model:

$$q_{bc} = (1 - P_c)q_{bcb} + (P_c)q_{bca} \quad (7)$$

$$q_{bca} = \alpha(\tau_* - \tau_{*c})^{1.5}\sqrt{Rgd^3} \quad (8)$$

$$q_{bcb} = \alpha(\tau_* - \tau_{*cb})^{1.5}\sqrt{Rgd^3} \quad (9)$$

$$\tau_{*cb} = \frac{\tau_{*c} r_{br}\sigma_{br}}{d}\left(\frac{d}{r_{br}\sigma_{br}}\right)^{b_r} \quad (10)$$

$$b_r = \frac{0.67}{1+exp(1.5-d/r_{br}\sigma_{br})} \quad (11)$$

where $q_{bca}$ is the transport capacity per unit width for sediment moving on purely alluvial bed and $q_{bcb}$ is the transport capacity per unit width for sediment moving on purely bedrock bed. $\tau_{*cb}$ is the dimensionless critical shear stress for grains on bedrock portions of the bed.

The models proposed by Inoue et al. (2014) and Johnson (2014) may seem rather similar in that they estimate the transport capacity of a mixed alluvial – bedrock surface. However, both models opt for different approaches when it comes to estimating hydraulic roughness. The model by Inoue et al. (2014) directly uses the hydraulic roughness, but the model by Johnson (2014) calculates the hydraulic roughness from the roughness (topographic unevenness) of the bed surface. The model by Inoue et al. (2014) needs measurements of observed bedrock hydraulic roughness, and the model by Johnson (2014) needs topographic bedrock roughness. In the model by Inoue et al. (2014), the macro roughness of the bed acts only when converting the alluvial layer thickness to the alluvial cover ratio. The macro roughness affects the temporal change of the alluvial cover ratio but does not affect the alluvial cover ratio in the dynamic equilibrium state. In addition, in the model by Johnson (2014), first, the sediment transport capacities for the bedrock and alluvial bed are separately calculated, then total transport capacity is

estimated using $P_c$. Whereas, in the model by Inoue et al. (2014), first, the total hydraulic roughness height is calculated using $P_c$, then total transport capacity is estimated using the total hydraulic roughness.

[** *This method for estimating $k_{sb}$ applies only to Johnson's model. The method of calculating the observed value of $k_{sb}$ is explained in the section 2.3*.]

### 1.6 Probabilistic Model

Turowski and Hodge (2017) proposed a probability-based model for prediction of cover on bedrock channels, and investigated the distribution of sediment on the bedrock. Because they mainly focused on the transformation between a point of view considering sediment masses and one considering sediment fluxes, they did not treat the interaction between the alluvial cover and the bed roughness. However, there is a possibility to capture the effects of bedrock roughness on the alluvial cover by adjusting the probability of grain entrainment and deposition included in the model. They proposed cover consisting of combined exponential and linear effects of sediment supply. They defined P as the probability that a grain will settle on exposed bed. Similar to the other models taking $q_{bs}$ and $q_{bc}$ into consideration, the value of P can range from 0 to 1. P depends on exposed area (1-$P_c$) and mass of sediment on bed ($M_s^*$), and it is given as:

$$d(1-Pc) = -P(1-Pc, M_s^*, ..)dM_s^* \tag{12a}$$

$$P_c = 1 - \left[1 + (1-\omega) ln\left\{1 - \left(1 - e^{-M_0^* q_{bs}}\right) q_{bs}\right\}\right]^{\left(\frac{1}{1-\omega}\right)} \tag{12b}$$

where $\omega$ is the exponent, $M_0^*$ is the dimensionless characteristic sediment mass obtained as follows:

$$M_0^* = \frac{3\sqrt{3}\tau_{*c}}{2\pi} \frac{(\tau_*/\tau_{*c}-1)^{1.5}}{(\tau_*/\tau_{*c})^{0.5}-0.7} \tag{13}$$

They suggested that on shorter time scales, the sediment cover follows a linear relationship with the sediment supply. Their model also provides two other analytical solutions (Equation 30, 31 in Turowski and Hodge, 2017), however we are employing Equation 12 in this study as the equation does not contain any parameter with obscure physical meaning and all the parameters can be calculated in laboratory or analytically.

We hereafter refer Sklar and Dietrich (2004) model as linear model, Turowski et al.'s model (2007) as exponential model, Inoue et al.'s model (2014) as macro roughness model, Meyer-Peter and Müller (MPM) based Johnson's model (2014) as surface roughness model and Turowski and Hodge's model (2017) as probabilistic model.

## 2 Experimental Method

### 2.1 Experimental Flume

The experiments were conducted in a straight channel at the Civil Engineering Research Institute for Cold Region, Sapporo, Hokkaido, Japan. The experimental channel was 22m long, 0.5m wide and had a slope of 0.01. The width-depth ratio was chosen to achieve no-sandbar condition (i.e., small width-depth ratio, 6.1 to 8.3 in our experiments). Chatanantavet and Parker (2008) conducted several flume experiments with sandbar condition (i.e., large width-depth ratio, 11 to 30 in their experiments) and suggested that the alluvial cover increases linearly to the ratio of sediment supply and transport capacity of the channel when the slope is less than 0.015. The formation of bars strongly depends on the width – depth ratio (e.g., Kuroki and Kishi, 1984; Colombini et al., 1987). Generally, neither alternate bars nor double-row bars are formed under conditions with width-depth ratio < 15.

In this study, we investigated the influence of bedrock roughness on the alluvial cover under conditions where the slope and width - depth ratio were small compared to the experiments of Chatanantavet and Parker (2008).

### 2.2 Bed characteristics and conditions

The channel bed consisted of hard mortar. In order to achieve different roughness conditions, the beds in Gravel30, Gravel50 and Gravel5 were embedded with gravel of different sizes. In Gravel30, the embedded particle size is 30 mm, in Gravel50 particle size of 50 mm is embedded and in Gravel5, 5 mm particle size is embedded.

We performed an additional 2 cases with net-installation on the riverbed. The net was made of plastic. An installed net on the riverbed can trap sediment during high flow, eventually protecting the bed from further erosion from abrading sediment (Kazuaki et al.,2015, in Japanese). A net of mesh size 30 mm X 30 mm was installed on the bed in Net4 and Net2. The height of the net was 4mm and 2 mm respectively. Figure 1 shows the experimental channel bed of all 5 runs.

For each bed roughness (example: Gravel50 series), a group of experiments with varying sediment supply were performed for different time durations.


**Figure 1: Initial channel bed for each run.**

### 2.3 Measurement of observed bedrock roughness

In order to measure the initial bed roughness (before supplying sand), a water discharge of 0.03 $m^3/s$ was supplied, and the water level was measured longitudinally at every 1 m at the centre of the channel. The hydraulic roughness height for bedrock ($k_{sb}$) was calculated using Manning – Strickler relation and Manning's velocity formula.

$$k_{sb} = \left(7.66 n_m \sqrt{g}\right)^6 \quad (14a)$$

$$n_m = \frac{1}{U} D^{2/3} {S_e}^{1/2} \quad (14b)$$

where $n_m$ is the Manning's roughness coefficient and $U$ is the average velocity ($U = Q/wD$ where $U$ is the water discharge, $w$ is the channel width, $D$ is the water depth), $S_e$ is the energy gradient.

In order to compare the hydraulic roughness height and the riverbed-surface unevenness height, the riverbed height before water flow was measured with a laser sand gauge. The measurements were taken longitudinally at every 5 mm. The measurements were taken at three points: 0.15 m away from the right wall, the centre of the channel, and 0.15 m away from the left wall. The standard deviation representing the topographic roughness $\sigma_{br}$ was obtained by subtracting the mean slope from the riverbed elevation (Johnson and Whipple; 2010).

### 2.4 Measurement of dimensionless critical shear stress on bedrock

To measure the dimensionless critical shear stress of grains on completely bedrock portion, i.e. $\tau_{*cb}$, 30 gravels of 5mm diameter each, were placed on the flume floor at intervals of 10 cm or more to make sure that there was no shielding effect between the gravels (there was shielding effect due to unevenness of the bedrock). Next, water flow was supplied at a flow discharge that no gravel moved, and was slowly increased to a flow discharge at which all the gravels moved. The water level and the number of gravels displaced were measured and recorded for each flow discharge. These measurements were performed for all the 5 bedrock surfaces.

We calculated the dimensionless shear stress $\tau_*(= DS_e/Rd)$, here $R$ is the specific gravity of the submerged sediment (1.65). We defined the critical shear stress was $\tau_{*cb}$ is the weight average of $\tau_*$ using the number of displaced gravels.

### 2.5 Validation of alluvial cover

Different amounts of gravel (5mm, hereafter called as sediment) was supplied manually while the flow rate was kept constant at 0.03 $m^3/s$. The alluvial cover ratio was measured once equilibrium state was achieved. Once the areal fraction became stable in qualitative observations and the variation of hydraulic roughness of mixed alluvial – bedrock bed $k_s$ calculated from the observed water depth was decreased despite sediment being supplied, we considered that the experiment has reached its equilibrium state. The sediment supply amounts and other experimental conditions for various cases are provided in Table 1. Each run has multiple cases, each with different sediment supply and time duration. Each case was performed unless the $P_c$ became constant. The gravels were supplied from Run-0 of no sediment to Run-4~5 of completely alluvial cover. The Run-0 with no sediment supply in each run represents the bedrock-roughness measurement experiment explained in section 2.3.

For each roughness condition, initially, we supplied sediment at the rate of $3.73 \times 10^{-5} m^2/s$ and observed the evolution of Pc. If Pc≈1, the sediment supply was approximately reduced by 1.5 times in the subsequent run, and then the sediment supply was further reduced to 2 times and 4 times in subsequent runs (example: Gravel30, Gravel50 and Net4). In roughness conditions where sediment supply of $3.73 \times 10^{-5} m^2/s$ resulted in Pc≈0, the sediment supply was increased by 1.25 or 1.5 times and 2 times in the subsequent runs (example: Gravel5 and Net2). However, for ease of understanding, we will present each experimental run in ascending order of sediment supply rate.

Equilibrium conditions were achieved after 2-4 hours of sediment supply. The alluvial cover was calculated at the end of the experiment, using black and white photographs of the flume by taking the ratio of the number of pixels. The water level was measured and recorded every hour at the centre of the channel, to calculate the hydraulic roughness during and at the end of the experiment. Bedrock topography with alluvial cover was also measured with a laser sand gauge. Since bedrock topography without alluvial cover has been measured in section 2.3, we can calculate the alluvial thickness from the difference of the two data.

**Table 1: Experimental Conditions.**

| Run | $k_{sb}$ (mm) | $k_{sb}/d$ | $q_{bs}$ ($\times 10^{-5}$m$^2$/s) | Time (hour) | $P_c$ | $D$ | $U$ | $Fr^{*1}$ | $k_s/d$ |
|---|---|---|---|---|---|---|---|---|---|
| Gravel30-0 | 48.0 | 9.6 | 0.00 | 0.25 | 0.00 | 0.082 | 0.74 | 0.82 | 9.6 |
| Gravel30-1 | | | 0.93 | 4.00 | 0.55 | 0.082 | 0.73 | 0.82 | 10.9 |
| Gravel30-2 | | | 1.87 | 4.00 | 0.75 | 0.082 | 0.74 | 0.82 | 6.9 |
| Gravel30-3 | | | 2.80 | 4.00 | 0.93 | 0.082 | 0.74 | 0.82 | 4.5 |
| Gravel30-4 | | | 3.73 | 4.00 | 0.99 | 0.082 | 0.73 | 0.82 | 1.8 |
| Gravel50-0 | 24.8 | 5.0 | 0.00 | 0.25 | 0.00 | 0.078 | 0.83 | 0.95 | 5.0 |
| Gravel50-1 | | | 0.93 | 4.00 | 0.20 | 0.077 | 0.79 | 0.91 | 3.6 |
| Gravel50-2 | | | 1.87 | 4.00 | 0.34 | 0.077 | 0.79 | 0.91 | 2.9 |
| Gravel50-3 | | | 2.80 | 4.00 | 0.46 | 0.074 | 0.82 | 0.97 | 2.7 |
| Gravel50-4 | | | 3.73 | 5.00 | 0.91 | 0.075 | 0.80 | 0.93 | 2.7 |
| Gravel5-0 | 3.8 | 0.8 | 0.00 | 0.25 | 0.00 | 0.063 | 0.95 | 1.21 | 0.8 |
| Gravel5-1 | | | 3.73 | 2.00 | 0.01 | 0.063 | 0.95 | 1.20 | 1.0 |
| Gravel5-2 | | | 5.60 | 2.00 | 0.03 | 0.060 | 1.00 | 1.30 | 1.1 |
| Gravel5-3 | | | 7.47 | 4.00 | 1.00 | 0.063 | 0.96 | 1.23 | 2.0 |
| Net4-0 | 36.3 | 7.3 | 0.00 | 0.25 | 0.00 | 0.077 | 0.78 | 0.90 | 7.3 |
| Net4-1 | | | 0.93 | 4.00 | 0.46 | 0.079 | 0.76 | 0.87 | 4.2 |
| Net4-2 | | | 1.87 | 4.00 | 0.62 | 0.079 | 0.76 | 0.87 | 4.1 |
| Net4-3 | | | 2.80 | 4.00 | 0.81 | 0.079 | 0.76 | 0.86 | 3.6 |
| Net4-4 | | | 3.73 | 5.00 | 0.99 | 0.078 | 0.77 | 0.89 | 3.2 |
| Net2-0 | 9.6 | 1.9 | 0.00 | 0.25 | 0.00 | 0.068 | 0.88 | 1.08 | 1.9 |
| Net2-1 | | | 3.73 | 4.00 | 0.06 | 0.068 | 0.88 | 1.08 | 1.9 |
| Net2-2 | | | 4.67 | 6.00 | 1.00 | 0.068 | 0.88 | 1.07 | 2.4 |
| Net2-3 | | | 5.60 | 4.00 | 1.00 | 0.068 | 0.88 | 1.07 | 3.1 |

*1: Froude number $Fr = u/(gD)^{0.5}$

## 3 Experimental results

### 3.1 Initial topographic roughness and hydraulic roughness

Figure 2 shows the relationship between the hydraulic roughness height of bedrock bed $k_{sb}$ and the topographic roughness height of bedrock bed $\sigma_{br}$. This figure suggests that Gravel30 with 30 mm sized embedded gravel, has the largest hydraulic roughness and Gravel5 with 5 mm sized embedded gravel has the lowest hydraulic roughness. Gravel50 embedded with 50 mm gravel has large topographical roughness error bars for the reason that, the large gravels were embedded randomly in the bed, resulting in unintended spatial variation in the unevenness of the channel bed. Although the hydraulic roughness tends to increase with an increase in topographical roughness, it has a large variation. This variation is due to the fact that the hydrological roughness height does not only depend on the topographical roughness but also on the arrangement of the unevenness.

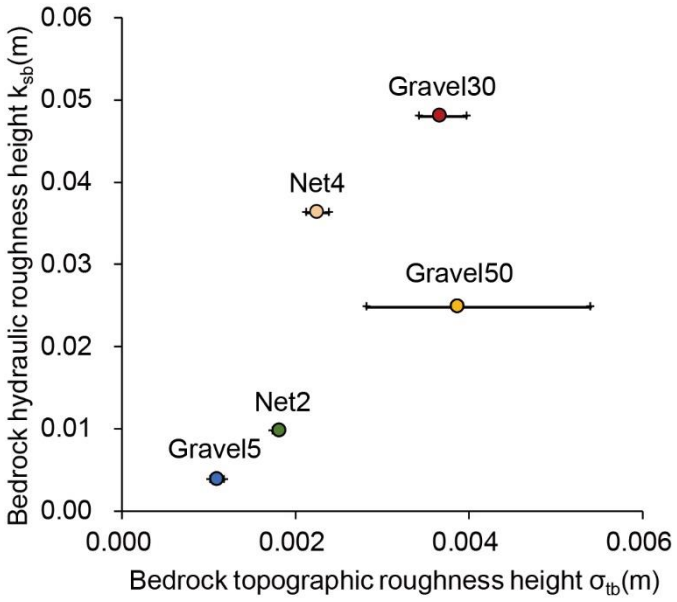


**Figure 2: Relationship between initial bed hydraulic roughness height and topographic roughness height. The black circles in the image represent the average values measured on the three data collection lines, and the error bars represent the minimum and maximum value.**

### 3.2 Relative roughness, sediment supply and alluvial cover

Figure 3 shows the channel bed after the experiments of the Gravel30 series (Gravel30-1, Gravel30-2, Gravel30-3 and Gravel30-4) with the highest relative roughness. Figure 4 shows the channel bed after the experiments of the Gravel5 series (Gravel5-1, Gravel5-2, Gravel5-3) which has the lowest relative roughness. In these two figures, we can compare Gravel30-4 and Gravel5-1 with equal sediment supply rates. The bed in Gravel30-4 is completely covered with sediment whereas the bed in Gravel5-1 has almost no accumulated sediment on the bed.

Figure 5 shows the relationship between alluvial-cover fraction $P_c$ and sediment supply per unit width $q_{bs}$. $P_c$ is obtained by dividing the sediment-covered area by the total area of the channel from photographs. The value of $P_c$ is 1 for a completely covered channel and 0 for a completely exposed bedrock bed. In Figure 5, if we compare Gravel30-4, Gravel50-4, Gravel5-1, Net4-4 and Net2-1, the cases with equal sediment supply rate of $3.73 \times 10^{-5}$ m$^2$/s, it can be observed that alluvial-cover fraction is increasing with an increase in the bedrock roughness. Moreover, in Gravel30 series, Gravel50 series and Net4 series with high relative roughness $k_{sb}/d$ (ratio of the hydraulic roughness height of bedrock bed $k_{sb}$ to the grain size $d$), $P_c$ is roughly proportional to the sediment supply rate $q_{bs}$. However, in Gravel5 series and Net2 series, which have lower $k_{sb}/d$ (relative roughness), $P_c$ shows hardly any increase when $q_{bs}$ is low (Gravel5-0, Gravel5-1, Gravel5-2, Net2-0, Net2-1) and when sediment supply ($q_{bs}$) increases (Gravel5-3, Net2-2), the bedrock suddenly transitions to completely alluvial bed.

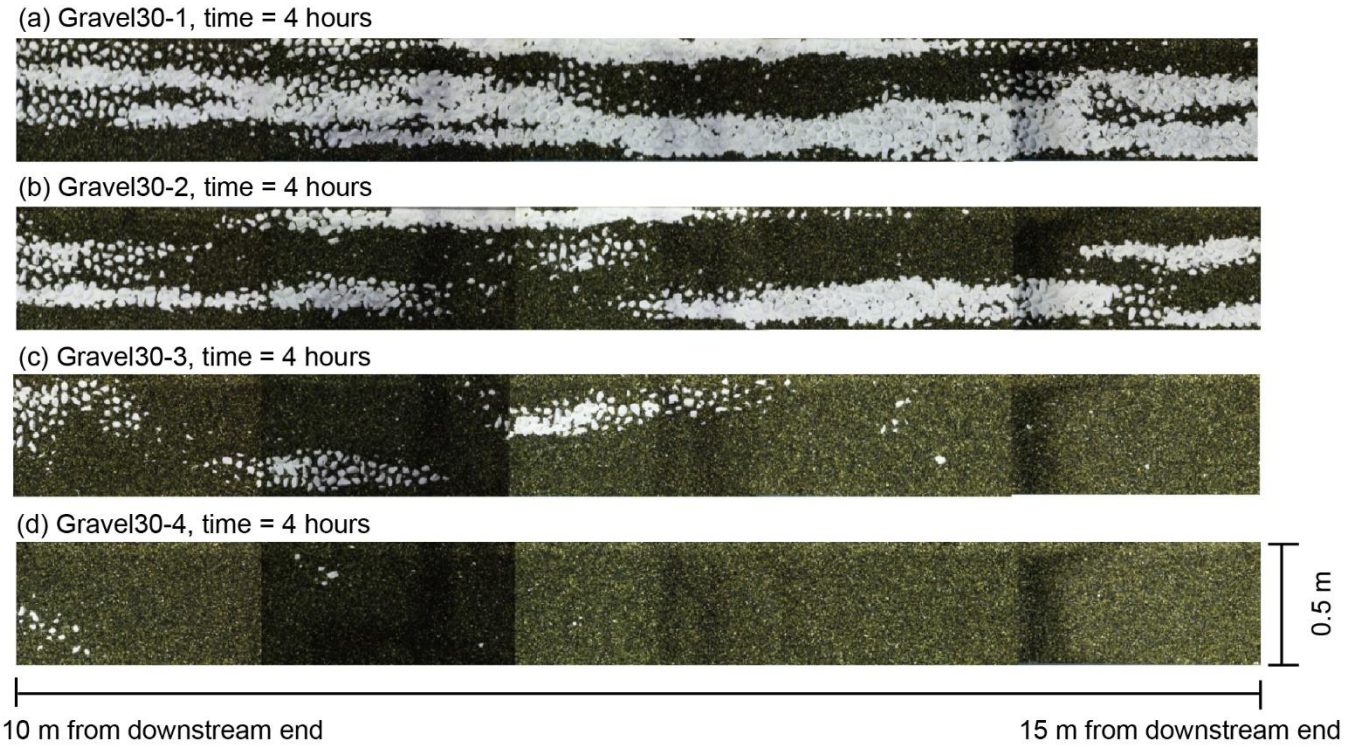


**Figure 3: Bedrock exposure in Gravel30 series at the end of the experiment. Initial bed had 30mm embedded particles. White bed represents exposed bedrock. Dark bed represents sediment covered bed.**

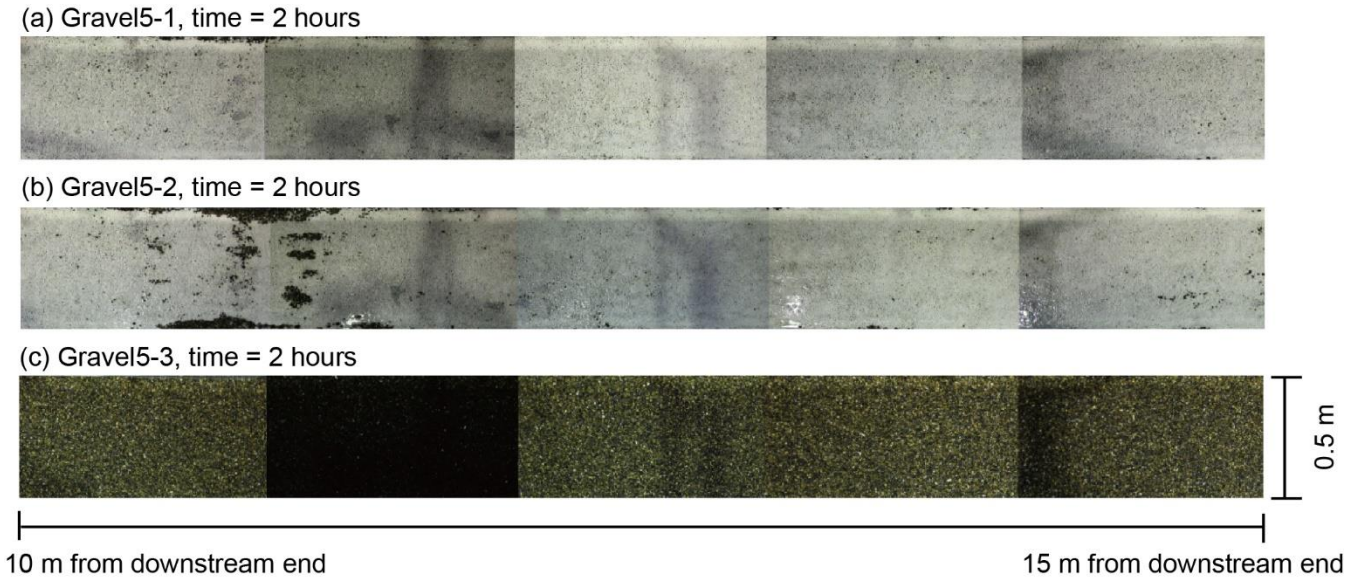


**Figure 4: Bedrock exposure in Gravel5 series at the end of the experiment. Initial bed had 5mm embedded particles.**

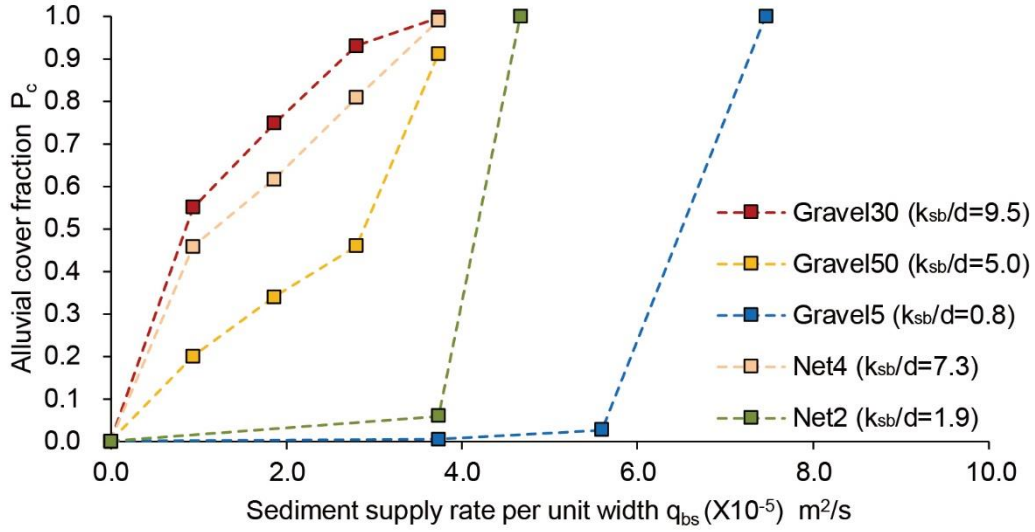


**Figure 5: Variation in alluvial cover fraction (Pc) with sediment supply.**

340

### 3.3 Relationship between gravel layer thickness and alluvial cover fraction

As explained in Section 1.5, the ratio of alluvial thickness $\eta_a$ to macro-roughness $L$ affects the temporal change of the alluvial cover ratio but does not affect the alluvial cover ratio in the dynamic equilibrium state. Thus, $\eta_a/L$ is not used in the model comparison in this study. However, we experimentally investigate $\eta_a/L$ because various numerical and theoretical models have employed alluvial cover as a function of relative alluvial thickness (Zhang et al., 2015; Inoue et al., 2014; Parker et al., 2013; Tanaka and Izumi, 2013; Nelson and Seminara, 2012)

$$P_c = \begin{cases} \eta_a/L & for\ \ 0 \le \eta_a/L \le 1 \\ 1 & for\ \ \eta_a/L > 1 \end{cases} \quad (15)$$

here, $\eta_a$ is the average thickness of the alluvial layer, $L$ is the macro-roughness height of the bedrock bed. Parker et al. (2013) define $L$ as the macroscopic asperity height of rough bedrock rivers $L_b$ ($\approx 2\sigma_{br}$). Tanaka and Izumi (2013) and Nelson and Seminara (2012) define $L$ as the surface unevenness of alluvial deposits on smooth bedrock river $L_a$ ($\approx d$). In this study, we define $L = 2\sigma_{br} + d$ so that it can cope with both smooth and rough bedrocks. Figure 6 shows the relationship between relative gravel layer thickness $\eta_a/L$ and alluvial cover ratio. The figure confirms that the alluvial cover ratio of the experimental result can be efficiently evaluated by Equation (15).

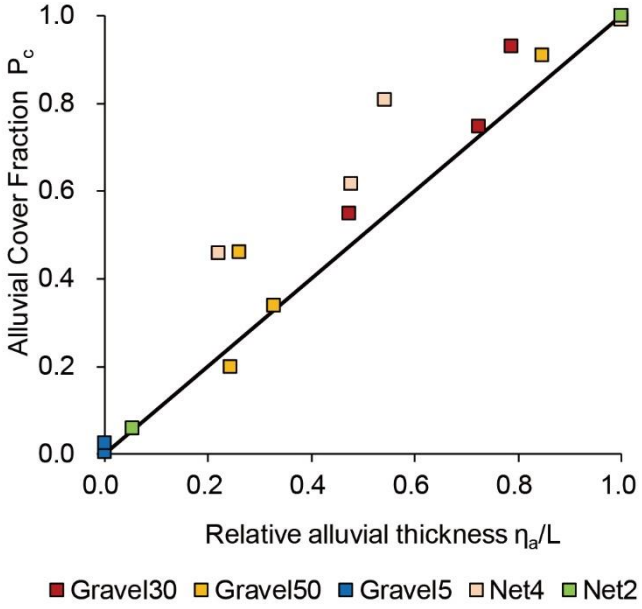


**Figure 6: Relationship between relative gravel layer thickness and alluvial cover. The black line represents the 1:1 line.**

### 3.4 Time series change of relative roughness

Figure 7 shows the change in relative roughness with time in Gravel30 and Gravel5 series. The red and blue points in Figure 7 show the alluvial cover fraction after water supply in Gravel30 and Gravel5 series, respectively.

In Run 1 series with a higher relative roughness, relative roughness decreased due to the increase in alluvial deposition and cover. In Run 3 series which has a lower initial relative roughness increased due to the increase in alluvial deposition and cover.

The relative roughness after the water supply is ~2 for both Gravel30-4 and Gravel5-3 while the alluvial cover fraction approaches 1. This value is almost the same as the relative roughness of flat gravel bed (about 1 to 4 times the particle size, generally about 2 times). This confirms that with an increase in alluvial cover, the relative roughness of the bed is determined by the gravel size.

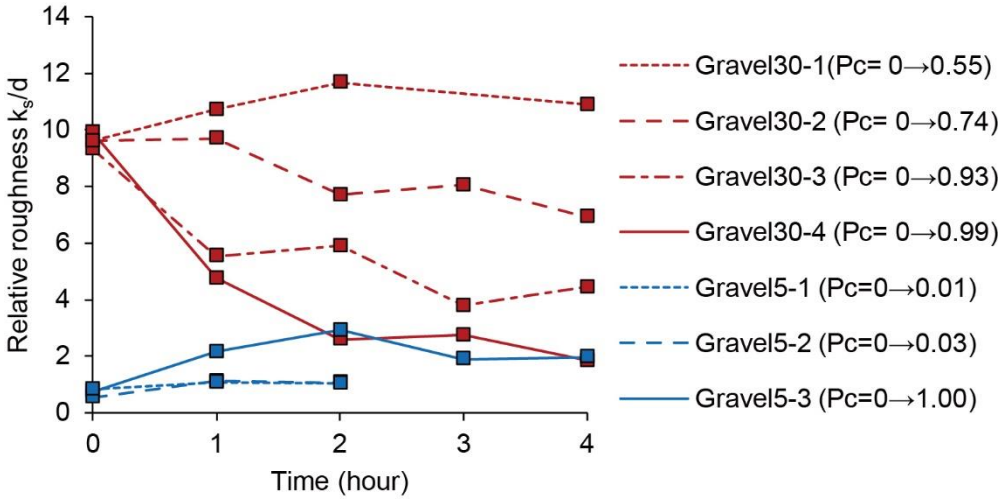


**Figure 7: Change in Relative roughness with time.**

### 3.5 Alluvial cover w.r.t relative roughness

Figure 8 shows the variation in $P_c$ with respect to relative roughness. In cases with lower initial relative roughness, example: Gravel 50 and Net2, the relative roughness is increasing with an increase in $P_c$. Whereas, in cases with higher initial relative roughness, Gravel30, Gravel5 and Net4, an increase in $P_c$ reduces the relative roughness. Besides, irrespective of the initial relative roughness, the bed tries to become completely alluvial as $P_c \approx 1$. Furthermore, irrespective of the initial relative roughness, an increase in $P_c$ forces each roughness condition to achieve a similar stabilised roughness. Also, several studies in the past have suggested that when bed consists of a uniform grain size and also comprises of bedload consisting of uniform and same size grains as the cover, the hydraulic roughness height ($k_s$) for such a bed is 1 to 4 times the grain diameter ($d$) (Inoue et al., 2014; Kamphuis, 1974; Parker, 1991) which is also the case in our experiments in Figure 8.

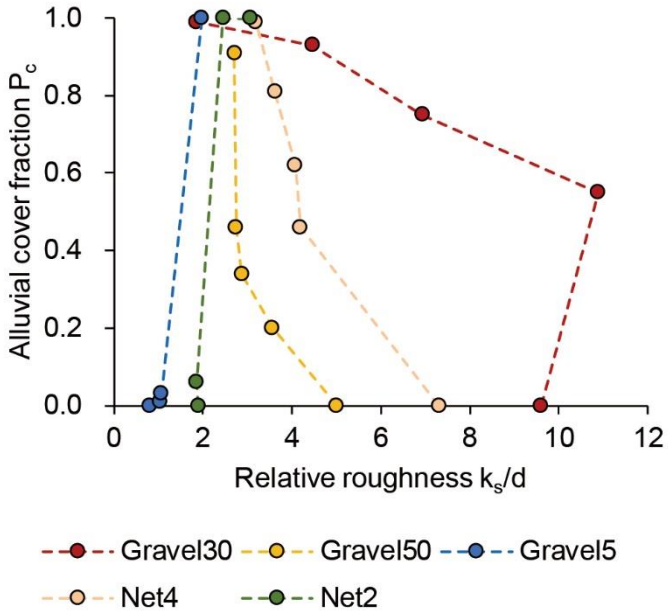


**Figure 8: Variations in $P_c$ with relative roughness.**

## 4 Discussion and Comparison of the Existing Models with Experimental Results

### 4.1 Calibrating $k_{\#D}$ and $r_{br}$

For the purpose of model comparisons with experimental results, we need to first calibrate Johnson's model parameters $k_{\#D}$ and rbr to minimize RMSD (root mean square deviation) of cover between experimental data and the model. When $k_{\#D} = 1$, it means the alluvial hydraulic roughness is proportional to the grain diameter size and is independent of the cover fraction. For our calculations, we have used $k_{\#D} = 4$ as applied in Johnson (2014). We also calibrate the exponential model's parameter $\varphi$ (Turowski et al, 2007). Table 2 provides the calibration values for $r_{br}$ and $\varphi$ for comparison of the model with our experimental results.

**Table 2: $r_{br}$ and $\varphi$ values for comparison with experimental results**

| | Observed $k_{sb}$ (mm) | Observed $\sigma_{br}$ (mm) | Adjusted $r_{br}$ ($k_{\#D}$=4) | Calculated $k_{sb}$ (mm, $k_{sb}$=$r_d$ $r_{br}\sigma_{br}$) | Adjusted $\varphi$ |
|---|---|---|---|---|---|
| Run 1 | 48.0 | 3.7 | 3.0 | 22.2 | 3.1 |
| Run 2 | 24.8 | 3.9 | 2.1 | 16.4 | 1.1 |
| Run 3 | 3.8 | 1.1 | 3.0 | 6.6 | 0.4 |
| Run 4 | 36.3 | 2.3 | 4.6 | 21.2 | 2.2 |
| Run 5 | 9.6 | 1.8 | 2.6 | 9.4 | 0.9 |

### 4.2 Relative Roughness and dimensionless critical shear stress

Figure 9 shows the relationship between the ratio of the hydraulic roughness height of bedrock bed $k_{sb}$ to the grain size $d$ ($k_{sb}/d$: referred to as the relative roughness in section 3.2) and the dimensionless critical shear stress over bedrock bed $\tau_{*cb}$. The Figure shows results obtained from Johnson (2014) (Eq. 10) and from Inoue et al. (2014) (Eq. 5) i.e. surface-roughness model and macro-roughness model, respectively.

According to Figure 9, the non-dimensional critical shear stress depends on the relative roughness to the power of 0.6. Besides, the results obtained from Eq. (5) of macro-roughness model are not compatible with the experimental results in the region where relative roughness of the bedrock bed is small. In this study, we used the power approximation shown below instead of Eq. (5) in the macro roughness model by Inoue et al. (2014).

$$\tau_{*c} = 0.03(k_s/d)^{0.6} \quad (16)$$

Likewise, the results obtained from Johnson's model (2014) (Eq. 10) (surface-roughness model) are consistent with our experimental results, but the model is inconsistent when the roughness is low.

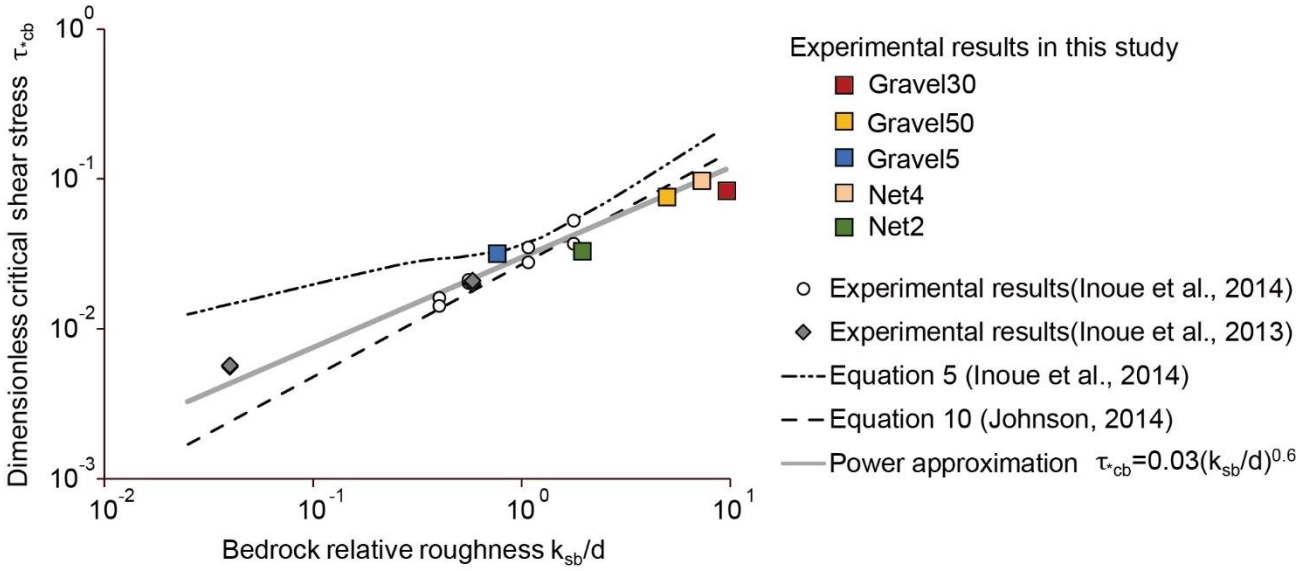


**Figure 9: Relationship between relative roughness and dimensionless critical shear stress. The black squares show the results of this experiment, the white circles show the results of investigation using the bedrock of Ishikari River in 2011 (Inoue et al., 2014), the grey rhombus represents a smooth aquifer floor (Inoue and Ito, 2013 (in Japanese)), the grey line shows the power approximation of all the experimental results. The dotted line shows the results from Eq. 5 proposed by Inoue et al. (2014). The black double dotted lines show the results obtained by Eq. 10 (Johnson, 2014). The grain size (*d*) in case of Inoue et al., (2013) is 5mm. and Inoue et al., 2014 used gravels sized: 12mm and 28mm.**

### 4.3 Predicting experimental results using the models

Figure 10 shows the comparison among experimental results presented in this paper, Sklar and Dietrich's linear model (2014), Turowski et al.'s exponential model (2007). This Figure suggests that the linear model is generally applicable to rough bed with relative roughness of 2 or more, but not to smooth bed with relative roughness less than 2 (Run 1, Run 2 and Run 4). As suggested by Inoue et al. (2014), in this study, "smooth bed" refers to the bed with roughness less than the roughness of supplied gravel (clast-smooth) and "rough bed" stands for the bed with roughness more that the roughness of the supplied gravel (clast-rough). The exponential model is also more suitable for a rough bed. Figure 11 shows the comparison of our observed experimental values with Inoue et al.'s macro-roughness model (2014) and Johnson's surface-roughness model (2014). It shows that the macro-roughness model proposed by Inoue et al. (2014) can predict the increasing alluvial cover for cases with high relative roughness, as well as the rapid alluviation and hysteresis (green shaded region) for cases with lower relative roughness (Run 3 and Run 5), without adjusting the roughness (explained in the following paragraph). The surface-roughness model proposed by Johnson (2014) also shows good agreement in predictions of alluvial cover and rapid alluviation and hysteresis if $k_{\#D}$ and $r_{br}$ are adjusted.

Figure 12 shows the comparison of experimental results with Turowski and Hodge's probabilistic model (2017). The model produces favourable results following some parameter adjustments. Because the probabilistic model (Turowski and Hodge,

2017) does not consider the effect of bedrock roughness on entrainment and deposition, the values of exponent $\omega$ and characteristic sediment mass $M_0^*$ needs to be adjusted by trial and error. The value of $\omega$ can be as high as 100 or 200 for Runs with rapid alluviation hysteresis, whereas it is as low as ~0.7 for other Runs.

In Figure 11, in Run 3 and Run 5 with relatively smooth beds, a rather scarce deposition was observed when sediment supply was low, and rapid alluviation occurred when sediment supply exceeded the transport capacity of the channel i.e. the bed was suddenly completely covered by alluvium. The reverse-line slopes produced by macro-roughness and surface-roughness models depict similar hysteresis relationship between alluvial cover and sediment supply i.e. sediment deposition occurs only for a certain range of sediment supply. The shaded portion shows that, as $q_{bs}/q_{bca}$ increases the cover does not increase unless it reaches a threshold ($q_{bs}/q_{bca}>1$, i.e. transport capacity over exposed bed is higher than transport capacity over fully covered bed), after which the cover increases abruptly, showing rapid alluviation. The green-shaded portion however is unstable between $P_c=0$ and $P_c=1$, i.e. it shows the hysteresis of rapid alluviation and rapid entrainment. As long as $q_{bs}>q_{bca}$ the value of $P_c$ will increase until it reaches 1, however if $q_{bs}$ becomes smaller than $q_{bca}$, $P_c$ will decrease until $P_c=0$ (rapid entrainment). For the bed to become alluviated again, $q_{bs}$ must reach a condition where $q_{bs}/q_{bca}>1$, in which case rapid alluviation will happen again. This phenomenon has also been observed in sufficiently steep channels, for slopes greater than 0.015 by Chatanantavet and Parker (2008). Hodge and Hoey (2016b) also suggested a similar relationship between sediment cover and sediment supply. However, our study shows that rapid alluviation occurs irrespective of the slope steepness, if roughness of the bed is less than the roughness of supplied gravel, i.e. when relative roughness is less than 2.

For investigating the influence of bed roughness on the alluvial cover in a bedrock channel with alternate bars. we also compared the experimental results of Chatanantavet and Parker (2008) with the model results of the physically based models including interaction between roughness and alluvial cover (i.e., Inoue et al., 2014; Johnson, 2014). Chatanantavet and Parker (2008) conducted experiments in a metallic straight channel with three different types of bedrock bed surfaces namely Longitudinal Grooves (LG), Random Abrasion Type 1 (RA1) and Random Abrasion Type 2 (RA2), where RA1 is smoother than RA2. They performed various cases for each type with varying slope range of 0.0115 – 0.03. They also varied the sediment supply rate and grain size (2mm and 7mm). The major difference between their experiment and our experiments is the width – depth ratio. The width-depth ratios of their experiments were 11 – 30, and thus allowed for the formation of alternate bars. In contrast, the width – depth ratios of our experiments were 6.1 – 8.3, as a result alternate bars usually do not develop. Although we can see alternate alluvial patches in Figure 5, their thickness was less than 1 cm, and the patches did not progress to alternate bars with large wave height. Figure 13 shows the comparison among the two models and Chatanantavet and Parker's experiment (2008). The experimental conditions are taken from Table 1 of Chatanantavet and Parker (2008). Figure 13a represents runs 2-C1 to 2-C4, Figure 13b represents runs 2-E1 to 2-E3, Figure 13c represents runs 3-A1 to 3-A5, Figure 13d represents runs 3-B1 to 3-B5, Figure 13e represents runs 1-B1 to 1-B4 (Chatanantavet and Parker 2008, Table 1). In case of the surface-roughness model, $k_{\#D} = 4$ is used, the bedrock surface roughness required for calculations is taken as mentioned in Table 1 Johnson (2014), $r_{br}$ is adjusted to minimize RMSD of cover between experiments and the model. In case of the macro-roughness model by Inoue et al. (2014), $k_{sb}$ is adjusted to minimize RMSD of cover. The two models can accurately predict the cover fraction and rapid alluviation for the experimental study conducted by Chatanantavet and Parker (2008).

A particularly important point of interest is the adjustment of hydraulic roughness value of the bedrock surface $k_{sb}$. In case of Chatanantavet and Parker's experiment, $k_{sb}$ ~ 0.4 mm to 3.5mm (Chatanantavet and Parker 2008, Table 1), whereas, in Johnson's surface-roughness model (2014), $k_{sb}$ $(= r_d r_{br} \sigma_{br})$ can be as much as 13 – 27 mm. Also, in the case of Inoue et al.'s macro-roughness model $k_{sb}$ is adjusted to 32 – 53 mm (Table 3).

**Table 3: Parameter calibration values for comparison with experimental results of Chatanantavet and Parker (2008)**

| Type | Slope | Observed $k_{sb}$ (mm) | $\sigma_{br}$ (mm) | Adjusted $r_{br}$ for the surface-roughness model $k_{\#D}$=4 | Calculated $k_{sb}$ in the surface-roughness model (mm, $k_{sb}= r_d\, r_{br}\sigma_{br}$) | Adjusted $k_{sb}$ for the macro-roughness model (mm) |
|---|---|---|---|---|---|---|
| LG | 0.02 | 0.4 | 6.7 | 1.8 | 24.1 | 42.0 |
| RA1 | 0.016 | 0.4 | 2.4 | 5.3 | 25.4 | 42.0 |
| | 0.03 | 0.4 | 2.4 | 5.7 | 27.4 | 53.0 |
| RA2 | 0.0115 | 3.5 | 2.7 | 2.5 | 13.5 | 32.0 |
| | 0.02 | 3.5 | 2.7 | 4.3 | 23.2 | 45.0 |

### 4.4 Differences and limitations

As mentioned earlier, the major difference between the macro-roughness model (Inoue et al., 2014) and surface-roughness model (Johnson., 2014) is the way the transport capacity is calculated. In case of the surface-roughness model (Johnson, 2014), first, the transport capacities for bedrock ($q_{bcb}$) and alluvial bed ($q_{bca}$) are separately calculated, then the total transport capacity ($q_{bc}$) is calculated for a range of cover fractions ($P_c$). Hence, in cases when $\tau_{*ca} < \tau_* < \tau_{*cb}$, the transport capacity over bedrock portion $q_{bcb} = 0$ and thereby the bedrock roughness hardly affects the alluvial cover fraction which can also be the reason for inconsistency between the surface-roughness model (Johnson, 2014) results and experimental study for Runs 1 and 4 in Figure 11 and RA2 Slope = 0.0115 in Figure 13. Whereas, in the case of macro-roughness model (Inoue et al., 2014), the critical shear stress takes into account the value of total hydraulic roughness, which depends on cover fraction, alluvial hydraulic roughness and bedrock hydraulic roughness. Hence, even when $\tau_*$ is small, the bedrock roughness tends to affect the cover fraction. The macro-roughness model (Inoue et al., 2014) is more efficient at dealing with clast-smooth surfaces.

Comparing the observed $k_{sb}$ with the adjusted $k_{sb}$ in the roughness models proposed by Inoue et al. (2014) and Johnson (2014), the adjusted $k_{sb}$ strongly depends on observed $k_{sb}$ in our experiments without alternate bars (Figure 14a), whereas, the adjusted $k_{sb}$ is not dependent on the observed $k_{sb}$ in experiments with alternate bars conducted by Chatanantavet and Parker (2008) (Figure 14b), suggests that bedrock roughness has a smaller effect on the alluvial cover in case of mixed alluvial – bedrock rivers with alternate bars. In such rivers, the bed slope may affect the alluvial cover fraction (Figure 14c). The roughness models are adjusted to produce the experimental results with alternate bars by fine-tuning $r_{br}$ and $k_{sb}$ values which must be determined by trial and error method. While this method can be applicable to laboratory-scale experiments, the model calibration is unfeasible for a large-scale channel or natural rivers. In general, the formation of alternate bars is barely reproduced with a one-dimensional model as introduced in this study. In the future, research to incorporate the effects of bars into a one-dimensional model, or analysis using a two-dimensional planar model (e.g., Nelson and Seminara, 2012; Inoue et al., 2016, 2017) is expected. Also, in order to deploy models on field-scale, they must take into account bank-roughness and its effects on shear stress and other hydraulic parameters. Ferguson (2019) argued that standard deviation of exposed bed is an effective way of roughness estimation, however, it needs further research on appropriating scaling.

Also, the probabilistic model proposed by Turowski and Hodge (2017) could reproduce experimental results but the model needed adjustment of $\omega$ and $M_0^*$ by trial and error, especially for cases involving rapid alluviation. The model however does not emulate the hysteresis for clast-smooth beds. Because the model does not include the effects of bed roughness yet, further alterations to take into account the effect of probability of grain entrainment and deposition can greatly extend the applicability of the model to natural bedrock rivers. In addition, recently, Turowski (2020) proposed a stochastic model that includes the

effects of bar formation, and further development is expected in the future. Taking into account the spatial variability in the tools effect (laboratory experiments by Bramante et al., 2020) will also take the models closer to field-scale studies.

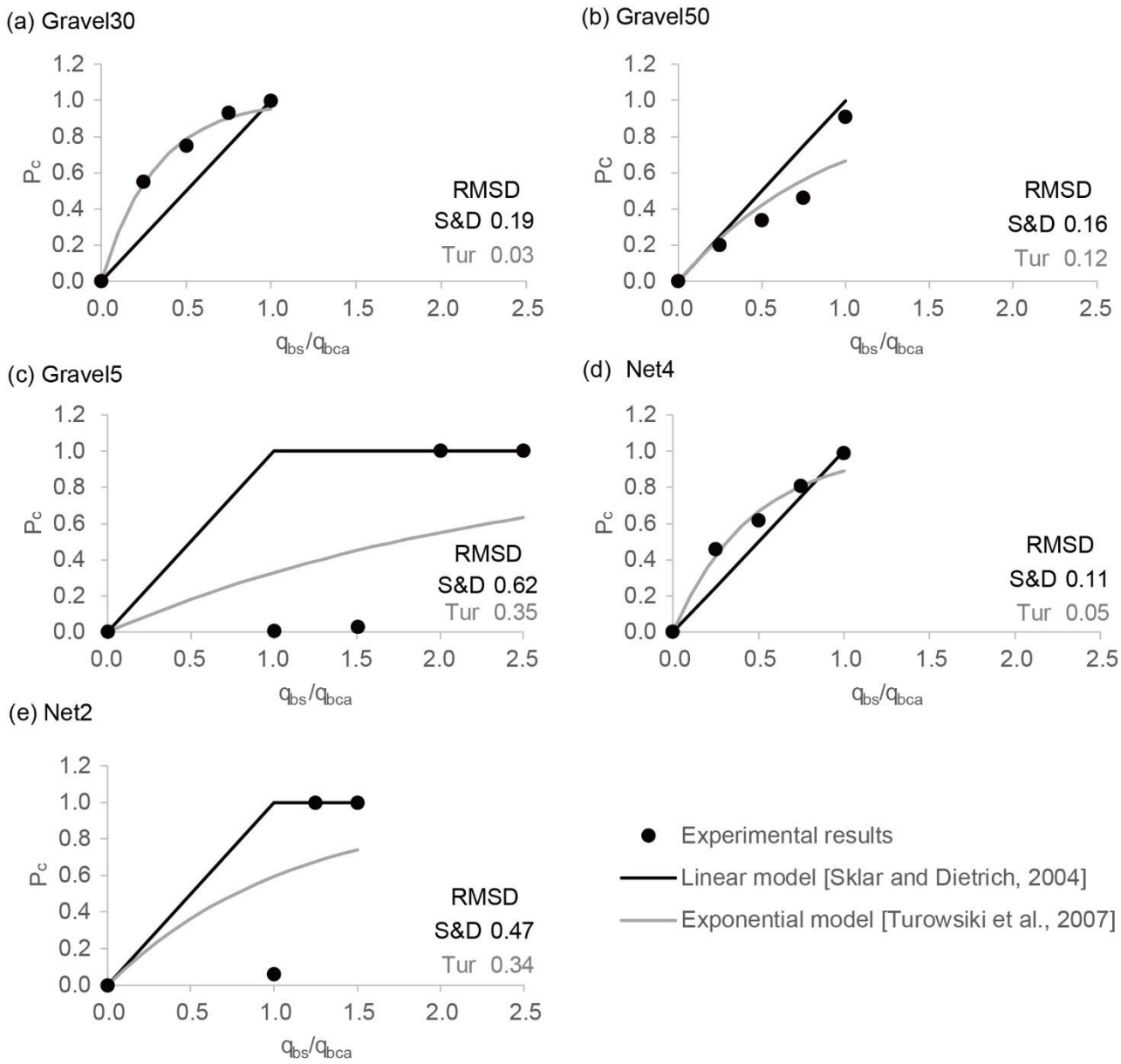


515 **Figure 10: Comparison of our experimental results, linear model by Sklar and Dietrich (2004) and exponential model by Turowski et al. (2007),**

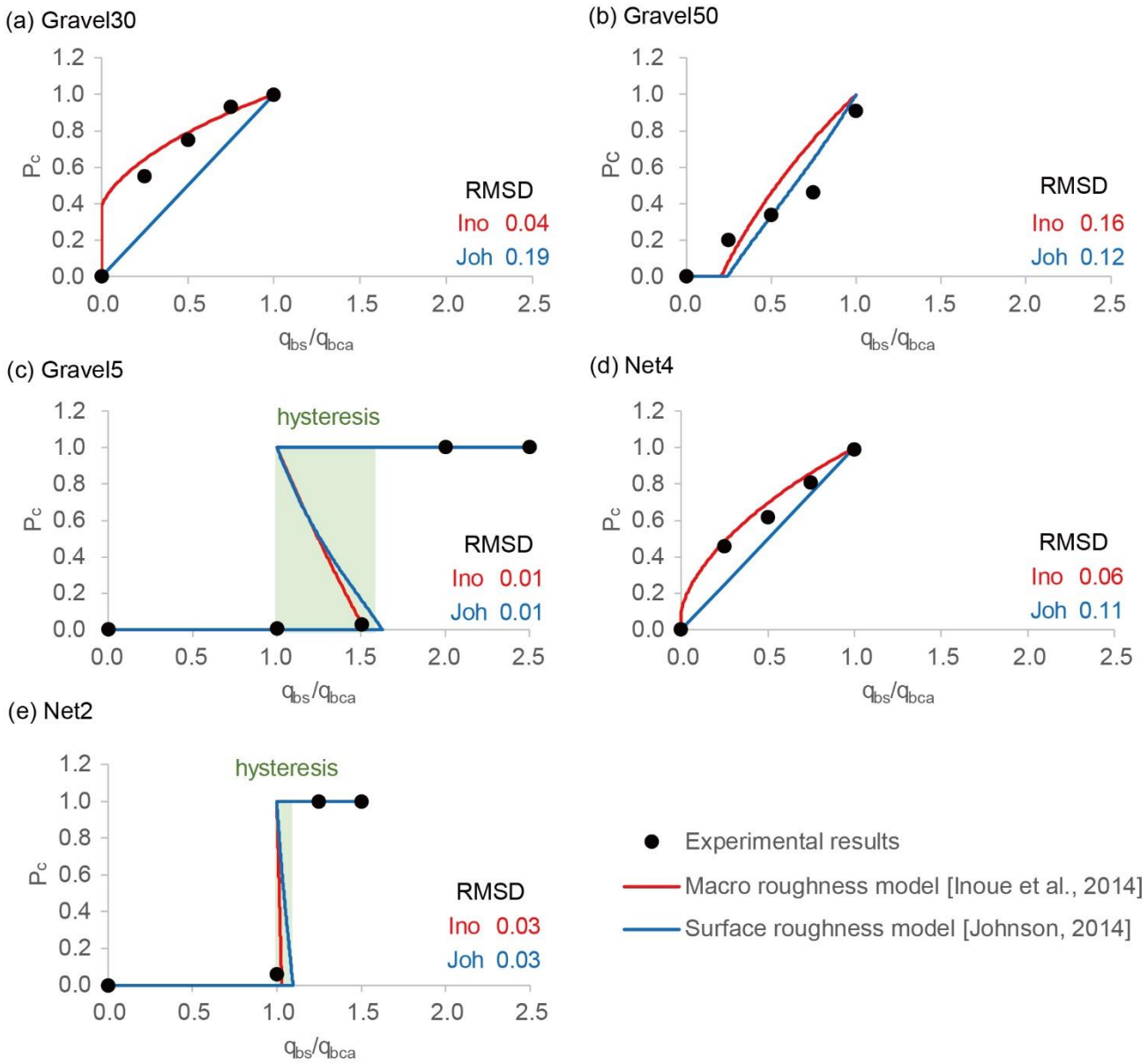


520 **Figure 11: Comparison of our experimental results with roughness models by Inoue et al. (2014) and Johnson (2014). The $r_{br}$ for the surface roughness model and the $\varphi$ for the exponential model are adjusted to minimize RMSD of the alluvial cover (see Table 2).**

525

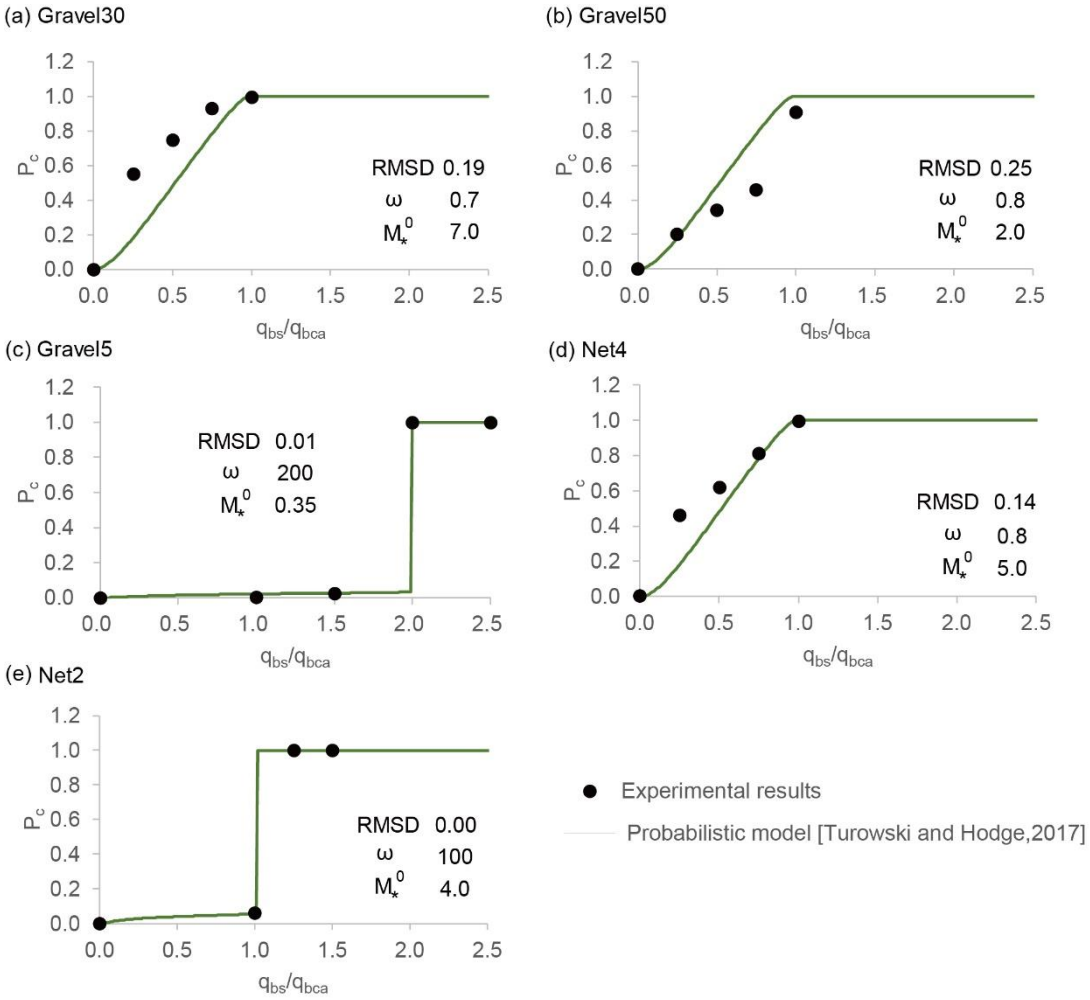


**Figure 12: Comparison of our experimental results with the probabilistic model proposed by Turowski and Hodge (2017).**

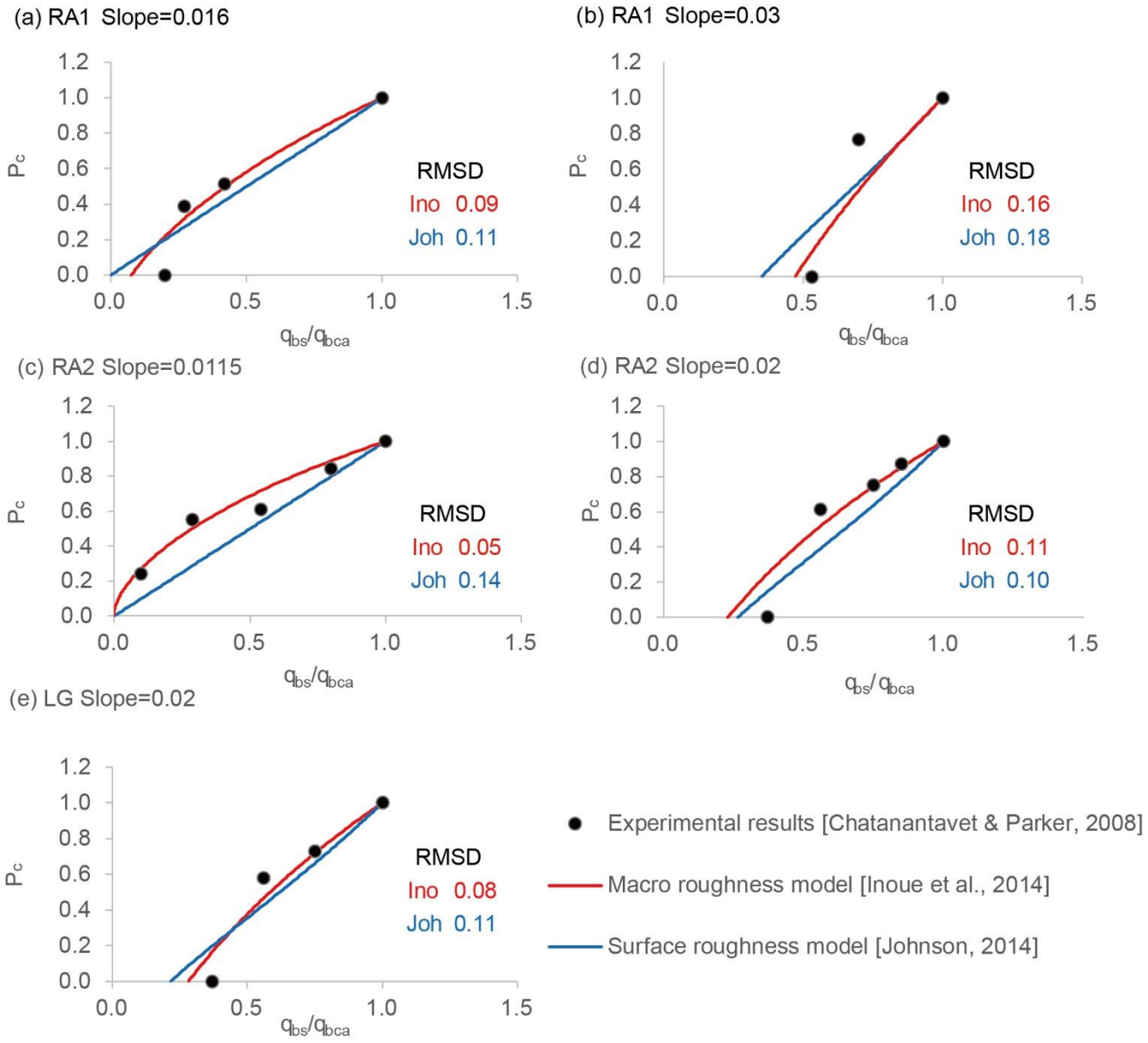


**Figure 13: Comparison of the experimental results (Chatanantavet and Parker, 2008) with the macro roughness model (Inoue et al., 2014) and the surface roughness model (Johnson, 2014). RA1, RA2 and LG represent the type of bedrock surface in the experiments conducted by Chatanantavet and Parker (2008); RA1 is Random Abrasion type 1, RA2 iss Random Abrasion type 2 and LG is Longitudinal grooves, respectively. The $r_{br}$ for the surface roughness model and the $k_{sb}$ for macro roughness model are adjusted to minimize RMSD of the alluvial cover (see Table 3).**

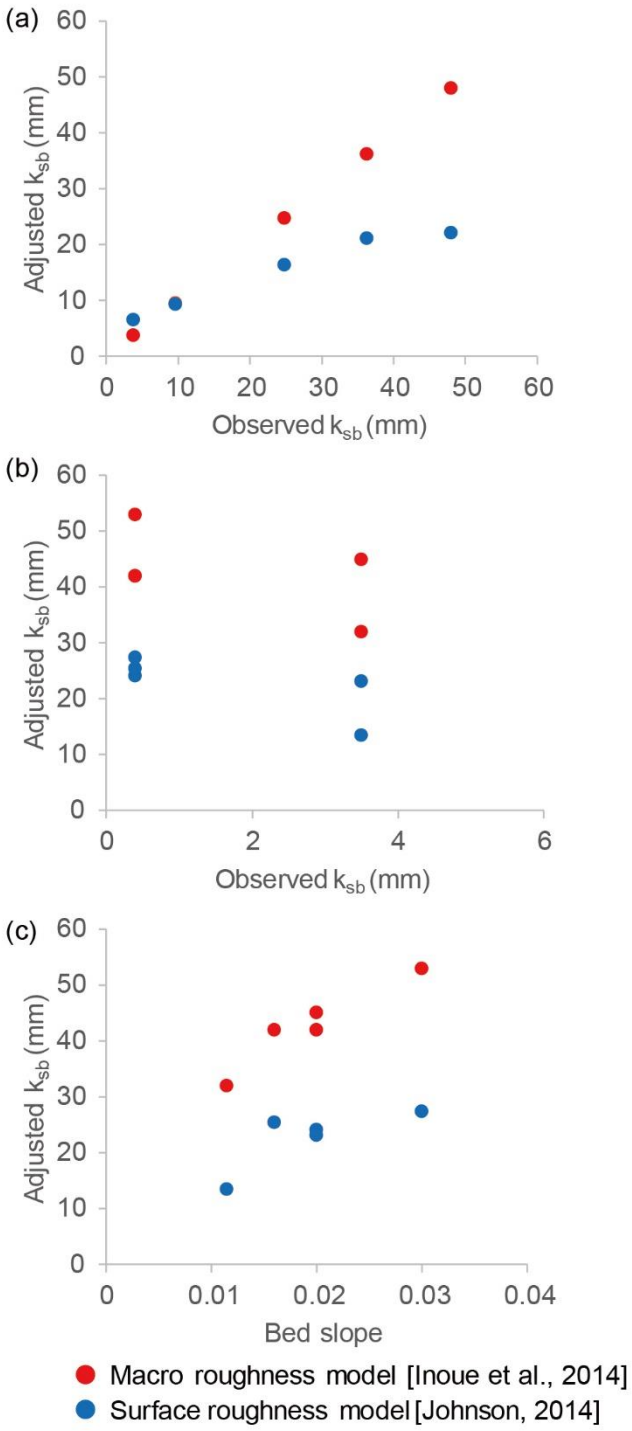


**Figure 14: (a) Comparison between adjusted and observed hydraulic roughness height of bedrock bed for our experiments. (b) Comparison between adjusted and observed hydraulic roughness height of bedrock bed for the experiments conducted by Chatanantavet and Parker (2008). (c) Sensitivity of adjusted $k_{sb}$ to bed-slope $S$ for experiments conducted by Chatanantavet and Parker (2008).**

## 5 Summary

Here we provide a review of models and studies focused at discovering the interaction between alluvial cover and bed roughness. For evaluating the previous models, we conducted laboratory-scale experiments with multiple runs of varying bed roughness and sediment supply. The experimental results show that the change in alluvial cover to the sediment supply rate is controlled by bedrock roughness to a great extent. When the bedrock hydraulic roughness is higher than the hydraulic roughness of the alluvial bed (i.e., clast-rough bedrock), the alluvial cover increases proportionately with the increase in sediment supply and then reaches an equilibrium state. However, in cases where bedrock roughness is lower than the roughness of the alluvial bed (i.e., clast-smooth bedrock), the deposition is insignificant unless sediment supply exceeds the transport capacity of the bedrock bed. When sediment supply exceeds the transport capacity, the bed abruptly covered by sediments and quickly reaches to completely alluvial bed.

We have also implemented the previous models for alluvial cover, i.e., the linear model proposed by Sklar and Dietrich (2004), the exponential model by Turowski et al. (2007), the macro-roughness model by Inoue et al. (2014), the surface-roughness model by Johnson (2014) and the probabilistic model by Turowski and Hodge (2017) in order to predict the experimental results. The linear model and exponential model are inefficient for cases with a clast-smooth bedrock specifically, they cannot predict the rapid-alluviation. The macro-roughness model (Inoue et al. 2014) and surface-roughness model (Johnson, 2014) can efficiently predict the rapid-alluviation and hysteresis for clast-smooth bedrock as well as the proportionate increase in alluvial cover for clast-rough bedrock. In particular, the macro-roughness model (Inoue et al. 2014) was able to reproduce the observed alluvial cover ratio without adjusting the parameters. The probabilistic model by Turowski and Hodge (2017) also needs parameter adjustments to make it sensitive to dynamic cover or rapid alluviation in clast-smooth bed, however, it does not reproduce the hysteresis.

We also tested the macro-roughness model (Inoue et al. 2014) and surface-roughness model (Johnson, 2014) for their capability to predict the experimental results observed by Chatanantavet and Parker (2008), in which the bedrock surface has alluvial alternate bar formations. Both models required significant parameter adjustments to reproduce the alluvial cover fraction. The two models do not include the 2-D effects caused by variable alluvial deposition and formation of bars on bedrock. Although models that extended the roughness model into a plane two-dimensional (e.g., Nelson and Seminara, 2012; Inoue et al., 2016) will be able to capture the bar formation in a bedrock river, these models require long time for simulation. Building a simpler model that can predict alluvial cover fraction with bar formation represents an exciting challenge in the future which contributes better understanding of long-time evolution of natural bedrock channel..

**Author Contribution:** Both authors contributed equally to the manuscript.

**Acknowledgements:** Data used in this publication is available in this paper itself or available in the papers referred (Chatanantavet and Parker, 2008 and Johnson 2014). In proceeding with this research, we received valuable comments from Professor Yasuyuki Shimizu, Professor Norihiro Izumi, and Professor Gary Parker. We would like to express our gratitude here. The authors would also like to thank Jens M Turowski, Rebecca Hodge and an anonymous referee for their constructive feedback that helped improve the earlier version of this paper.

**Notations:**

| | |
|---|---|
| $\alpha$ | bedload transport coefficient |
| $b_r$ | exposure function by Johnson (2014) |
| $d$ | particle size (m) |
| $D$ | water depth (m) |

| | |
|---|---|
| g | gravitational acceleration (9.81 m/s$^2$) |
| $k_s$ | hydraulic roughness height (m) |
| $k_{sa}$ | hydraulic roughness height of purely alluvial bed (m) |
| $k_{sb}$ | hydraulic roughness height of purely bedrock bed (m) |
| $k_{\#D}$ | dimensionless alluvial roughness |
| $\kappa$ | Karman constant |
| $l$ | flume length (m) |
| $L$ | macro-roughness height of bedrock bed (m) |
| $M_0^*$ | dimensionless sediment mass |
| $n_m$ | Manning's roughness coefficient (m$^{-1/3}$s) |
| $\eta_a$ | average thickness of alluvial layer (m) |
| $P_c$ | mean areal fraction of alluvial cover |
| $\varphi$ | cover factor proposed by Turowski et al. (2007) |
| $q_{bs}$ | sediment supply rate per unit width (m$^2$/s) |
| $q_{bc}$ | transport capacity per unit width (m$^2$/s) |
| $q_{bca}$ | transport capacity per unit width for sediment moving on purely alluvial bed (m$^2$/s) |
| $q_{bcb}$ | transport capacity per unit width for sediment moving on purely bedrock bed (m$^2$/s) |
| $Q$ | water discharge (m$^3$/s) |
| $r_d$ | scaling coefficient for *d* and hydraulic roughness length |
| $r_{br}$ | fitting parameter that scales bedrock roughness to *d* |
| $R$ | specific gravity of sediment in water (1.68) |
| $S$ | Bed slope |
| $S_e$ | energy gradient |
| $\tau_*$ | dimensionless shear stress |
| $\tau_{*c}$ | dimensionless critical shear stress |
| $\tau_{*ca}$ | dimensionless critical shear stress for grains on purely alluvial bed |
| $\tau_{*cb}$ | dimensionless critical shear stress for grains on purely bedrock bed |
| $U$ | depth averaged velocity (m/s) |
| $w$ | flume width (m) |
| $\omega$ | Exponent by Turowski and Hodge (2017) |
| $\sigma_{br}$ | topographic roughness height of purely bedrock bed (m) |

**References**


Aubert, G., Langlois, V. J., and Allemand, P.: Bedrock incision by bedload: insights from direct numerical simulations, Earth Surf. Dynam.,4, 327–342, https://doi.org/10.5194/esurf-4-327-2016, 2016.

Beer, A. R., and Turowski J. M.: Bedload transport controls bedrock erosion under sediment-starved conditions, Earth Surf. Dyn., 3, 291–309, doi:10.5194/esurf-3-291-2015., 2015.

Beer, A. R., Kirchner, J. W., and Turowski, J. M.: Graffiti for science – erosion painting reveals spatially variable erosivity of sediment-laden flows, Earth Surf. Dynam., 4, 885–894, https://doi.org/10.5194/esurf-4-885-2016, 2016.

Beer, A. R., Turowski, J. M., and Kirchner, J.W.: Spatial patterns of erosion in a bedrock gorge, J. Geophys. Res.-Earth, 122, 191–214, https://doi.org/10.1002/2016JF003850, 2017.

Bramante, J.F., Perron, J.T., Ashton, A.D., and Donnelly, J.P.,:Experimental quantification of bedrock abrasion under oscillatory flow: Geology, 48, https://doi.org/10.1130/G47089.1, 2020.

Byerlee, J.D.: Friction of rocks, Pure and Applied Geophysics 116 (4–5), 615–626,1978.

Chatanantavet, P., and Parker G.: Experimental study of bedrock channel alluviation under varied sediment supply and hydraulic conditions, Water Resour. Res., 44, W12446, doi:10.1029/2007WR006581, 2008.

Chepil, W. S.: The Use of Evenly Spaced Hemispheres to Evaluate Aerodynamic Forces on a Soil Surface, Transactions A.G.U., 39(3), 397-404, 1958.

Colombini, M., Seminara, G., & Tubino,: M. Finite-amplitude alternate bars, J. Fluid Mech., 181, 213– 232. doi: 10.1017/S0022112087002064, 1987

Cook, K.L., Turowski, J.M., Hovius, N.: A demonstration of the importance of bedload transport for fluvial bedrock erosion and knickpoint propagation. Earth Surf. Process. Landforms 38, 683–695. https://doi.org/10.1002/esp.3313, 2013

Cowie, P. A., Whittaker A. C., Attal M., Roberts G., Tucker G. E., and Ganas A.: New constraints on sediment-flux-dependent river incision: Implications for extracting tectonic signals from river profiles, Geology, 36(7), 535–538, doi:10.1130/g24681a.1., 2008.

Egiazaroff, I. V.: Calculation of non-uniform sediment concentrations, J. Hydraul. Div. Am. Soc. Civ. Eng., 91, 225–247. 1965.

Ferguson, R. I., Hardy, R. J., and Hodge, R. A. : Flow resistance and hydraulic geometry in bedrock rivers with multiple roughness length scales. Earth Surf. Process. Landforms, 44: 2437– 2449. https://doi.org/10.1002/esp.4673, 2019.

Fernández R, Parker G, Stark CP.: Experiments on patterns of alluvial cover and bedrock erosion in a meandering channel. Earth Surface Dynamics 7, 949-968, https://doi.org/10.5194/esurf-7-949-2019, 2019.

Finnegan, N. J., Sklar, L. S., & Fuller, T. K.: Interplay of sediment supply, river incision, and channel morphology revealed by the transient evolution of an experimental bedrock channel, Journal of Geophysical Research, 112, F03S11. https://doi.org/10.1029/2006JF000569, 2007.

Fuller, T. K., Gran, K. B., Sklar, L. S., & Paola, C.: Lateral erosion in an experimental bedrock channel: The influence of bed roughness on erosion by bed load impacts. Journal of Geophysical Research: Earth Surface, 121, 1084–1105. https://doi.org/10.1002/2015JF003728, 2016.

Gilbert, G. K.: Report on the Geology of the Henry Mountains: Geographical and Geological Survey of the Rocky Mountain Region, , U.S. Gov. Print. Off., Washington, D. C., 160, doi:10.5962/bhl.title.51652, 1877.

Hancock GS, Anderson RS.: Numerical modeling of fluvial strath-terrace formation in response to oscillating climate, Geological Society of America Bulletin, 114, 1131- 1142, https://doi.org/10.1130/0016-7606(2002)114<1131:NMOFST>2.0.CO;2, 2002.

Hobley, D. E. J., Sinclair, H. D., Mudd, S. M., and Cowie, P. A.: Field calibration of sediment flux dependent river incision, J. Geophys. Res., 116, F04017, https://doi.org/10.1029/2010JF001935, 2011.

Hodge, R. A., and Hoey, T. B. Upscaling from grain-scale processes to alluviation in bedrock channels using a cellular automaton model, J. Geophys. Res., 117, F01017, doi:10.1029/2011JF002145, 2012.

Hodge, R. A., and Hoey T. B.: A Froude-scaled model of a bedrock-alluvial channel reach: 1. Hydraulics, J. Geophys. Res. Earth Surf., 121, 1578–1596, doi:10.1002/2015JF003706, 2016a.

Hodge, R. A., and Hoey T. B.: A Froude-scaled model of a bedrock alluvial channel reach: 2. Sediment cover, J. Geophys. Res. Earth Surf., 121, 1597–1618, doi:10.1002/2015JF003709, 2016b.

Hodge, R. A., Hoey, T. B., and Sklar, L. S.: Bed load transport in bedrock rivers: The role of sediment cover in grain entrainment, translation, and deposition, J. Geophys. Res., 116, F04028, doi:10.1029/2011JF002032, 2011.

Hodge, R. A., Hoey, T. B., Maniatis, G., and Leprêtre, E.: Formation and erosion of sediment cover in an experimental bedrock-alluvial channel, Earth Surf. Proc. Land., 41, 1409–1420, https://doi.org/10.1002/esp.3924, 2016.

Inoue, T., and Ito A.: The relationship between roughness, critical Shear stress and sediment transport capacity on soft bedrock surface, Proceedings of the 68th Annual Conference of the Japan Society of Civil Engineers, II-072, 2013.

Inoue T.; Iwasaki T.; Parker G., Shimizu Y., Izumi N., Stark C. P., and Funaki J.: Numerical Simulation of Effects of Sediment Supply on Bedrock Channel Morphology. Journal of Hydraulic Engineering,142(7), 04016014- 1-11, doi:10.1061/(asce)hy.1943-7900.0001124, 2016.

Inoue, T., Izumi, N., Shimizu, Y., & Parker, G.: Interaction among alluvial cover, bed roughness, and incision rate in purely bedrock and alluvial-bedrock channel. Journal of Geophysical Research: Earth Surface, 119, 2123–2146. https://doi.org/10.1002/2014JF003133, 2014.

Inoue, T., Nelson, J. M.: An experimental study of longitudinal incisional grooves in a mixed bedrock–alluvial channel. Water Resour. Res, 56, e2019WR025410. doi:10.1029/2019WR025410, 2020.

Inoue, T., Parker, G., and Stark, C. P.: Morphodynamics of a bedrock-alluvial meander bend that incises as it migrates outward: approximate solution of permanent form. Earth Surf. Process. Landforms, 42, 1342– 1354, doi:10.1002/esp.4094., 2017a.

Inoue, T., Yamaguchi, S.. and Johnson, J. M.: The effect of wet-dry weathering on the rate of bedrock river channel erosion by saltating gravel, Geomorphology, 285(15), 152-161. doi.org/10.1016/j.geomorph.2017.02.018, 2017b.

Jansen, J. D., Fabel, D., Bishop, P., Xu, S., Schnabel, C., and Codilean, A. T.: Does decreasing paraglacial sediment supply slow knickpoint retreat?, Geology, 39, 543–546, doi:10.1130/G32018.1, 2011.

Johnson, J. P. L.: A surface roughness model for predicting alluvial cover and bed load transport rate in bedrock channels, J. Geophys. Res., 119, 2147–2173, https://doi.org/10.1002/2013JF003000, 2014

Johnson, J. P. and Whipple, K. X.: Feedbacks between erosion and sediment transport in experimental bedrock channels, Earth Surf. Proc. Land., 32, 1048–1062, https://doi.org/10.1002/esp.1471, 2007.

Johnson, J. P. L., and Whipple K. X.: Evaluating the controls of shear stress, sediment supply, alluvial cover, and channel morphology on experimental bedrock incision rate, J. Geophys. Res., 115, F02018, doi:10.1029/2009JF001335, 2010.

Johnson, J. P. L., Whipple K. X., Sklar L. S., and Hanks T. C.: Transport slopes, sediment cover, and bedrock channel incision in the Henry Mountains, Utah, J. Geophys. Res., 114, F02014, doi:10.1029/2007JF000862, 2009.

Johnson, J. P. L., Whipple, K. X., and Sklar, L. S.: Contrasting bedrock incision rates from snowmelt and flash floods in the Henry Mountains, Utah, Geological Society of America Bulletin,122(9–10), 1600–1615. https://doi.org/10.1130/b30126.1, 2010.

Kamphius, J. W.: Determination of sand roughness for fixed beds, J. Hydraul. Res., 12(2), 193–203, doi:10.1080/00221687409499737, 1974.

Kazuaki M., Inoue T., Shimizu Y.: Suppression method of soft rock erosion by using "net cover effect" and verification in real river, Advances in River Engineering, Vol.21, 165-170, 2015.

Kuroki, M., & Kishi, T.: Regime criteria on bars and braids in alluvial straight channels, Proc. Japan Soc. Civil Eng., 342, 87-96. doi: 10.2208/jscej1969.1984.342_87 (in Japanese), 1984.

Lague, D.: Reduction of long-term bedrock incision efficiency by short term alluvial cover intermittency, J. Geophys. Res.-Earth, 115, F02011, https://doi.org/10.1029/2008JF001210, 2010.

Meyer-Peter, E., and Müller R.: Formulas for bed-load transport, in Proceedings, Second Congress, International Association for Hydraulic Structures Research, Stockholm, 39–64, 1948.

Mishra, J., Inoue, T., Shimizu, Y., Sumner, T., & Nelson, J. M.: Consequences of abrading bed load on vertical and lateral bedrock erosion in a curved experimental channel, Journal of Geophysical Research: Earth Surf., 123, 3147– 3161. https://doi.org/10.1029/2017JF004387, 2018.

Moore RC.: Origin of inclosed meanders on streams of the Colorado Plateau, Journal of Geology 34, 29-57, https://www.jstor.org/stable/30063667, 1926.

Nelson, P. A., and Seminara G.: A theoretical framework for the morphodynamics of bedrock channels, Geophys. Res. Lett., 39, L06408, doi:10.1029/2011GL050806, 2012.

Nelson, P. A., Bolla Pittaluga, M., and Seminara, G.: Finite amplitude bars in mixed bedrock-alluvial channels, J. Geophys. Res.-Earth, 119, 566–587, https://doi.org/10.1002/2013JF002957, 2014.

Parker, G.: Selective sorting and abrasion of river gravel. 1: Theory, J. Hydraul. Eng., 117(2), 131–149, doi:10.1061/(ASCE)0733-9429(1991)117:2(131, 1991.

Parker, G., Fernández, R., Viparelli, E., Stark, C. P., Zhang, L., Fu, X., Inoue, T., Izumi, N., and Shimizu, Y.: Interaction between waves of alluviation and incision in mixed bedrock-alluvial rivers, Advances in River Sediment Research, Proc. of 12th International Symposium on River Sedimentation, ISRS, 615-622, 2013.

Scheingross, J.S., Brun, F., Lo, D.Y., Omerdin, K., and Lamb, M.P.: Experimental evidence for fluvial bedrock incision by suspended and bedload sediment: Geology, 42, 523–526, https://doi .org/10.1130/G35432.1. 2014,

Shepherd, R. G., and Schumm, S. A.: Experimental study of river incision, Geol. Soc. Am.Bull., 85, 257-268, 1974.

Shepherd, R. G.: Incised river meanders: Evolution in simulated bedrock, Science, 178, 409–411, https://doi.org/10.1126/science.178.4059.409, 1972.

Shobe, C. M., Tucker, G. E., and Barnhart, K. R.: The SPACE 1.0 model: a Landlab component for 2-D calculation of sediment transport, bedrock erosion, and landscape evolution, Geosci. Model Dev., 10, 4577–4604, https://doi.org/10.5194/gmd-10-4577-2017, 2017.

Sklar, L. S., and Dietrich W. E.: River longitudinal profiles and bedrock incision models: Stream power and the influence of sediment supply, in Rivers Over Rock: Fluvial Processes in Bedrock Channels, Geophys. Monogr. Ser., vol. 107, edited by K. Tinkler and E. E. Wohl, pp. 237–260, AGU, Washington, D. C., doi:10.1029/GM107p0237, 1998.

Sklar, L. S. and Dietrich, W. E.: Sediment and rock strength controls on river incision into bedrock, Geology 29, 1087–1090, https://doi.org/10.1130/0091-7613(2001)029<1087:SARSCO>2.0.CO;2, 2001.

Sklar, L. S., and Dietrich, W. E.: A mechanistic model for river incision into bedrock by saltating laboratory-scale, Water Resour. Res., 40, W06301, 2004.

Sklar, L. S., & Dietrich, W. E.: The role of sediment in controlling bedrock channel slope: Implications of the saltation-abrasion incision model. Geomorphology, 82(1–2), 58–83. https://doi..org/10.1016/j.geomorph.2005.08.019, 2006.

Tamaki, S., Takuya, I., Yasuyuki, S.,: The influence of bed slope change on erosional morphology, Journal of JSCE, 2019, 7(1), 15-21, Released January 20, 2019, Online ISSN 2187-5103, https://doi.org/10.2208/journalofjsce.7.1_15, 2019.

Tanaka, G., and Izumi N.: The Bedload Transport Rate and Hydraulic Resistance in Bedrock Channels Partly Covered with Gravel, Journal of the Japan Society of Civil Engineers B1 (Hydraulic Engineering), Vol. 69, No. 4, I_1033-I_1038, 2013.

Turowski, J. M.: Stochastic modeling of the cover effect and bedrock erosion, Water Resour. Res., 45, W03422, doi:10.1029/2008WR007262, 2009.

Turowski, J. M.: Alluvial cover controlling the width, slope and sinuosity of bedrock channels, Earth Surf. Dynam., 6, 29–48, https://doi.org/10.5194/esurf-6-29-2018, 2018.

Turowski, J. M.: Mass balance, grade, and adjustment timescales in bedrock channels, Earth Surf. Dynam., 8, 103–122, https://doi.org/10.5194/esurf-8-103-2020, 2020

Turowski, J. M. and Bloem, J.-P.: The influence of sediment thickness on energy delivery to the bed by bedload impacts, Geodin. Acta, 28, 199–208, https://doi.org/10.1080/09853111.2015.1047195, 2016.

Turowski, J. M. and Hodge, R.: A probabilistic framework for the cover effect in bedrock erosion, Earth Surf. Dynam., 5, 311–330, https://doi.org/10.5194/esurf-5-311-2017, 2017.

Turowski, J. M., and Rickenmann D.: Tools and cover effects in bedload transport observations in the Pitzbach, Austria, Earth Surf. Processes Landforms, 34, 26–37, doi:10.1002/esp.1686., 2009

Turowski, J. M., Lague D., and Hovius N.: Cover effect in bedrock abrasion: A new derivation and its implications for the modeling of bedrock channel morphology, J. Geophys. Res., 112, F04006, doi:10.1029/2006JF000697, 2007.

Turowski, J.M., Hovius, N., Meng-Long, H., Lague, D., Men-Chiang, C.: Distribution of erosion across bedrock channels. Earth Surface Processes and Landforms 33, 353–363. https://doi.org/10.1002/esp.1559, 2008a.

Turowski, J. M., Hovius, N., Wilson, A., and Horng, M.-J.: Hydraulic geometry, river sediment and the definition of bedrock channels, Geomorphology, 99, 26–38, https://doi.org/10.1016/j.geomorph.2007.10.001, 2008b.

Turowski, J. M., Badoux, A., Leuzinger, J., and Hegglin, R.: Large floods, alluvial overprint, and bedrock erosion, Earth Surf. Proc. Land., 38, 947–958, https://doi.org/10.1002/esp.3341, 2013.

Whitbread, K., Jansen, J., Bishop, P., and Attal, M.: Substrate, sediment, and slope controls on bedrock channel geometry in postglacial streams, J. Geophys. Res., 120, 779–798, https://doi.org/10.1002/2014JF003295, 2015.

Wilcock, P. R., and Crowe J. C.: Surface-based transport model for mixed-size sediment, J. Hydraul. Eng. Asce, 129(2), 120–128, doi:10.1061/(asce)0733-9429(2003)129:2(120), 2003.

Yamaguchi S., Inoue T., Akahori R., Sato D., Shimizu Y., Izumi N.: Analysis of bedload collision velocity near a knickpoint using PTV Method, Journal of Japan Society of Civil Engineers, Ser. B1 (Hydraulic Engineering), 74(5), I_1153-I_1158, https://doi.org/10.2208/jscejhe.74.5_I_1153, (released December 05, 2019 in Japanese), 2018.

Yanites, B. J., Tucker G. E., Hsu H. L., Chen C. C., Chen Y. G., and Mueller K. J.: The influence of sediment cover variability on long-term river incision rates: An example from the Peikang River, central Taiwan, J. Geophys. Res., 116, F03016, doi:10.1029/2010JF001933, 2011.

Zhang, L., Parker, G., Stark, C. P., Inoue, T., Viparelli, E., Fu, X., and Izumi, N.: Macro-roughness model of bedrock–alluvial river morphodynamics, Earth Surf. Dynam., 3, 113–138, https://doi.org/10.5194/esurf-3-113-2015, 2015.